

Turbulent flux variability and energy balance closure in the TERENO prealpine observatory: a hydrometeorological data analysis

Mohsen Soltani¹ · Matthias Mauder¹ · Patrick Laux¹ · Harald Kunstmann^{1,2}

Received: 7 November 2016 / Accepted: 24 July 2017 / Published online: 29 July 2017
© Springer-Verlag GmbH Austria 2017

Abstract The temporal multiscale variability of the surface heat fluxes is assessed by the analysis of the turbulent heat and moisture fluxes using the eddy covariance (EC) technique at the TERrestrial ENvironmental Observatories (TERENO) prealpine region. The fast and slow response variables from three EC sites located at Fendt, Rottenbuch, and Graswang are gathered for the period of 2013 to 2014. Here, the main goals are to characterize the multiscale variations and drivers of the turbulent fluxes, as well as to quantify the energy balance closure (EBC) and analyze the possible reasons for the lack of EBC at the EC sites. To achieve these goals, we conducted a principal component analysis (PCA) and a climatological turbulent flux footprint analysis. The results show significant differences in the mean diurnal variations of the sensible heat (H) and latent heat (LE) fluxes, because of variations in the solar radiation, precipitation patterns, soil moisture, and the vegetation fraction throughout the year. LE was the main consumer of net radiation. Based on the first principal component (PC1), the radiation and temperature components with a total mean contribution of 29.5 and 41.3%, respectively, were found to be the main drivers of the turbulent fluxes at the study EC sites. A general lack of EBC is observed, where the energy imbalance values amount 35, 44, and 35% at the Fendt, Rottenbuch, and Graswang sites, respectively. An average energy balance ratio (EBR) of 0.65 is obtained in the region. The

best closure occurred in the afternoon peaking shortly before sunset with a different pattern and intensity between the study sites. The size and shape of the annual mean half-hourly turbulent flux footprint climatology was analyzed. On average, 80% of the flux footprint was emitted from a radius of approximately 250 m around the EC stations. Moreover, the overall shape of the flux footprints was in good agreement with the prevailing wind direction for all three TERENO EC sites.

1 Introduction

Energy exchange between the land surface and the atmosphere is one of the crucial processes in any ecosystem (Berry and Dennison 1993). The surface turbulent fluxes are influenced both by the characteristics of the airflow and the structures of the underlying surface (Wyngaard 1990). The eddy covariance (EC) technique is the most direct way to estimate turbulent fluxes within the atmospheric boundary layer in any ecosystem (Swinbank 1951; Baldocchi et al. 1988; Verma 1990; Mauder and Foken 2006; Mauder et al. 2006). Its main challenges include system design, implementation, and processing of a large volume of data (Stull 1988; Foken 2009; Foken et al. 2010; Burba 2013). Via the EC technique, flux footprint information can be assessed (Schmid 1994) and quasi continuous flux measurements can be aggregated across different time scales, i.e., at hourly, daily, seasonal, and annual time scales (Wofsy et al. 1993; Baldocchi et al. 2001; Cava et al. 2008; Nakai et al. 2006). Moreover, the general characteristics of hydrometeorological variability and canopy exchange processes can be identified (Foken et al. 2011).

A multitude of experimental research has been conducted on the measurements of the daily, monthly, and seasonal variations of heat, water vapor, and CO_2 exchanges over heterogeneous lands in different ecosystems using the EC technique,

✉ Mohsen Soltani
mohsen.soltani@kit.edu

¹ Karlsruhe Institute of Technology (KIT/IMK-IFU), Institute of Meteorology and Climate Research,
82467 Garmisch-Partenkirchen, Germany

² Institute of Geography, University of Augsburg,
86150 Augsburg, Germany

such as cropland sites (e.g., Xu et al. 2011; Schmidt et al. 2011; Wizemann et al. 2014), forest environments (e.g., Launiainen et al. 2005; Sanchez et al. 2010), grasslands and paddy fields (e.g., Du et al. 2006; Hao et al. 2007; Gao et al. 2009; Moderow et al. 2009; Wang et al. 2010; Wohlfahrt et al. 2010; Li et al. 2013), and tropical and savanna areas (e.g., Merquiol et al. 2002; Steven et al. 2005; Mauder et al. 2007).

Currently, there are not many research studies on the surface energy and water flux variations for the prealpine region in the literature. Here, we present an analysis of a 2-year dataset of the EC measurements (2013–2014) over three experimental sites situated in prealpine and mountainous areas in southern Germany. Previous work in this region has focused on the impact of climate change on the runoff generation and hydrological aspects of Ammer river catchment (Kunstmann et al. 2004; Ott et al. 2013), greenhouse gas fluxes (Unteregelsbacher et al. 2013), water and energy flux observation and modeling (Kunstmann et al. 2013; Hingerl et al. 2016), soil-atmosphere exchange of N_2O and CH_4 (Wang et al. 2014), biosphere-atmosphere exchange of greenhouse gases (Wolf et al. 2017; Zeeman et al. 2017), and the evaluation purposes of semi-empirical energy balance closure (EBC) parameterizations (Eder et al. 2014). Since the diurnal and daily flux variability is represented by the data, our focus is set on the characterization of the monthly and seasonal variability of the water and energy fluxes, as well as the EBC between the study sites. Therefore, the objectives of this study are to quantify:

- 1) the surface energy and water fluxes variability, i.e., the spatiotemporal variations of the sensible and latent heat fluxes, soil moisture contents, and the energy partitioning conditions, the main drivers of the turbulent heat fluxes,
- 2) the EBC and residual energy, as well as the possible reasons for the lack of EBC at the TERENO prealpine EC sites.

2 Site characterization and measurement setup

2.1 Geography and climate

The TERrestrial ENvironmental Observatories (TERENO) prealpine region is located in southern Germany, where three EC stations are established in the areas of Fendt, Rottenbuch, and Graswang. Geographically, the Fendt site is within the northern part of the region and it is recognized as the TERENO prealpine super site, while the Rottenbuch and Graswang sites are located in the middle and southern parts of the region, respectively (See Fig. 1). The elevation ranges between 543 m in the north and 2129 m a.s.l. in the southern regions. The climate of the region is cool-temperate and humid. The mean annual air temperature is approximately 7–

8 °C in the alpine foreland and approximately 4–5 °C in the southern mountainous region. The northern area of the region receives an annual mean precipitation of approximately 1100 mm, while the summits of the Ammer Alps in the southern regions receive approximately 2000 mm. Maximum precipitation is in June and July (Kunstmann et al. 2006). Summer rains are characterized by convective events, causing a high variability in the location and intensity of rainfall. The main prevailing wind flow at individual stations is shown in Fig. 1. More details about the characteristics of the TERENO prealpine EC sites are provided in Table 1.

2.2 Data processing

The calculation of turbulent prealpine fluxes was done using the TK3 eddy covariance software. TK3 is able to perform all of the post-processing of turbulence measurements to produce the turbulent fluxes (Mauder and Foken 2015). It includes all necessary corrections and tests (Lee et al. 2004, Aubinet et al. 2012). The basic principle of the EC measurements is that the vertical flux is calculated as a covariance between the concentration of a scalar (e.g., air temperature and water vapor) and the vertical wind velocity measured at the same point in space and time (Mauder and Foken 2015). The turbulent fluxes of sensible heat (H) and latent heat (LE) can be calculated as (Kaimal and Finnigan 1994):

$$H = \bar{\rho} C_p \overline{w'T'} \quad (1)$$

$$LE = \bar{\rho} L_v \overline{w'q'} \quad (2)$$

where ρ , C_p , and L_v denote the density of air (kg/m^3), the specific heat of air ($J/kg\ K$), and latent heat of evaporation (J/kg), respectively. W' , T' , and q' are the fluctuations in the vertical wind component (m/s), air temperature (°C), and specific humidity, respectively. For more information regarding the calculation of turbulent fluxes and quality control (QC) using the TK3 software, refer to Mauder et al. (2013) and Mauder and Foken (2015).

The energy balance ratio (EBR) or the relative EBC (Aubinet et al. 1999) remains unclosed at most EC sites (e.g., Panin et al. 1998; Lamaud et al. 2001; Turnipseed et al. 2002; Wilson et al. 2002; Meyers and Hollinger 2004; Oncley et al. 2007; Hendricks Franssen et al. 2010; Stoy et al. 2013; Imukova et al. 2016). The energy storage change in the upper layer of the soil can be as high as $40\ W/m^2$, which can amount up to $\sim 20\%$ of the net radiation (Culf et al. 2004). Our soil heat flux (G) plates were buried at 8-cm depth to avoid disturbances, e.g., by losing contact with underlying soil and/or water accumulation below the plates (Sanchez et al. 2010). Thus, the soil heat storage in the above 8-cm depth was added to G to calculate EBR properly. The soil heat storage and the heat capacity were calculated according to the PlateCal

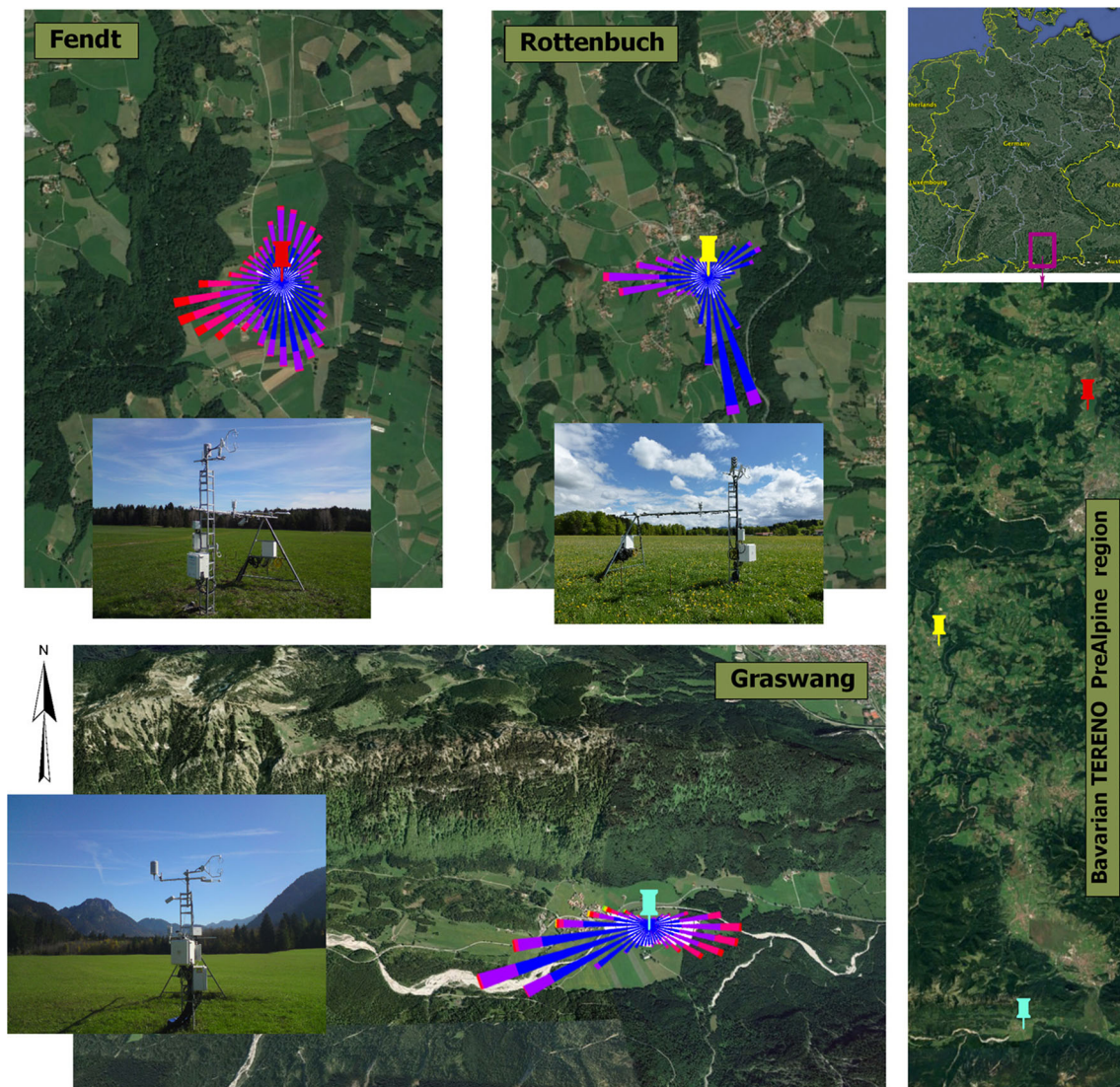


Fig. 1 Satellite images of the EC sites in the TERENO prealpine region (the approximate landscape area is $10 \text{ km} \times 40 \text{ km}$) in southern Germany are shown at the maps on the *right*, and the pins in the maps on the *left* indicate the approximate location of each EC site (the approximate flux

footprint area is $2.5 \text{ km} \times 5 \text{ km}$). The wind-rose diagrams are also overlaid (with the wind speed ranging from 1 to 11 m s^{-1} identified by the *colors* from *blue* to *red*, respectively). The prevailing background vegetation type is grassland for the three sites

approach of Liebenthal et al. (2006) and De Vries (1963), respectively. The volumetric fraction of organic matter at the Fendt EC site is approximately 30%. Accordingly, the half-hourly EBR for each site was calculated as (Stoy et al. 2013):

$$\text{EBR} = \frac{\sum(LE + H)}{\sum(Rn - G)} \quad (3)$$

with LE denoting the latent heat flux (W/m^2), H the sensible heat flux (W/m^2), Rn the net radiation (W/m^2), and G the soil heat flux (W/m^2) at the surface (Harazono et al. 1998; Burba et al. 1999).

In this study, a rain-free half-hourly dataset was collected in order to calculate the EBR. This is because open-path systems perform poorly during rainfall. Therefore, such

periods must be excluded from the dataset to calculate the EBC (Culf et al. 2004). The measurements by the enclosed-path systems may also be compromised, in general, when water is sucked into the sampling tube or when condensation occurs leading to severe damping of the humidity fluctuations (Kabat et al. 2003). However, at the Rottenbuch eddy covariance site, a rain-cap is used at the inlet of the enclosed-path gas analyzer in order to prevent this sucking of water during rain events and a heating at a rate of 5 W/m is applied to prevent condensation. Generally, the EC measurement is less reliable during rainy periods; turbulence cannot develop properly under these conditions. Therefore, no matter what instruments are used, data recorded during rainfall periods do not fulfill one of the basic requirements of the EC technique.

Table 1 EC site description at the TERENO prealpine region. Soil type characteristics and analysis of soil texture are according to Pütz et al. (2016)

| Site name | Fendt | Rottenbuch | Graswang |
|---|-----------------------------|-----------------------------|------------------------------------|
| Location | 47.831° N, 11.061° E | 47.730° N, 10.061° E | 47.571° N, 11.032° E |
| Elevation | 598 m | 770 m | 860 m |
| Slope | < 5° | < 5° | < 5° |
| Climate | Cool-temperate and humid | Cool-temperate and humid | Cool-temperate and humid |
| Mean annual air temperature | 9.3 °C | 8.6 °C | 7.0 °C |
| Mean annual precipitation | 962 mm | 1047 mm | 1464 mm |
| Vegetation type | Grassland | Grassland | Grassland |
| Soil type (texture: sand/silt/clay (%)) | Cambic Stagnosol (27/43/30) | Cambic Stagnosol (26/45/29) | Fluvic Calcaric Cambisol (9/39/52) |
| Canopy height range | 5–30 cm | 5–45 cm | 5–35 cm |

To determine the turbulent flux drivers at the study sites, a principal component analysis (PCA) is applied. PCA is a technique that is used to summarize the information (i.e., the total variation it contains) in a dataset described by multiple variables and can be applied to produce linear combinations of the variables that are mutually uncorrelated. In other words, PCA reduces the dimensionality of a multivariate dataset. This is achieved by transforming the initial variables into a new small set of variables without losing the most important information in the original dataset. These new variables correspond to a linear combination of the originals and are called principal components (PCs). The PCs are ranked in that way that PC1 explains the largest fraction of the variance in a dataset, PC2 the second largest, etc. (Abdi and Williams 2010).

The main goals of our PCA include the following: to identify hidden patterns in the hydrometeorological dataset, reduce the dimensionality of the data by removing the noise and redundancy in the data, rank the importance of single variables within this multivariate dataset, and finally to identify and group correlated variables. In this study, the *prcomp* and *fviz_pca* functions from the built-in *R stats* and *factoextra* packages were used to perform and visualize the PCA, respectively (R Core Team 2017). The procedure of the PCA includes the following steps:

- 1) Preprocessing of the dataset: first, the data were centered by subtracting the mean from each variable. Second, the data were scaled in order to have a unit variance.
- 2) Calculation of the covariance matrix of the preprocessed data.
- 3) Calculation of the eigenvectors and eigenvalues of the covariance matrix: the numbers on the diagonal of the diagonalized covariance matrix are the eigenvalues of the covariance matrix (large eigenvalues correspond to large variances). The directions of the new rotated axes are called the eigenvectors of the covariance matrix.
- 4) Dimension reduction and selection of PCs: eigenvectors were ordered by eigenvalues from the highest to the

lowest. The number of chosen eigenvectors is then the number of dimensions of the new dataset.

- 5) Computation of the new dataset: the transpose of the selected eigenvectors (PCs) were multiplied by the transpose of the original dataset.

Our PCA technique followed closely the mathematical formulation as given in Jolliffe (2002), Dray (2008), Abdi and Williams (2010), and Lay (2012).

2.3 Micrometeorological measurements

The instruments for measuring the radiation components and also the turbulent fluxes at the surface layer were installed on three towers in the TERENO prealpine region. The EC instruments were installed on a station 3.5 m above the surface at all three sites. The turbulent fluxes were measured with a 3-D sonic anemometer (CSAT3, Campbell Scientific Inc., Logan, UT), oriented towards the prevailing wind direction along with an open-path gas analyzer. All signals for the sensors were logged to a data logger (CR3000, Campbell Scientific Inc., Logan, UT) at a rate of 20 Hz and were averaged for a half-hourly period. All the required procedures for the corrections and QC of the turbulent fluxes were applied (Mauder et al. 2013), such as coordinate rotation by the double rotation method (Wilczak et al. 2001), sonic temperature Schotanus correction (Schotanus et al. 1983), frequency response corrections (Moore 1986), WPL correction (Webb et al. 1980), and QC following Foken et al. (2004). Simultaneous to the flux measurements, environmental and hydrometeorological data were measured at a 1-min resolution and averaged for 10-min intervals. The instrumentation between all three sites is almost identical, except for an enclosed-path infrared CO₂ and H₂O analyzer (LI7200, LI-COR Biosciences Inc., Lincoln, NE) in Rottenbuch instead of the open-path instruments (LI7500, LI-COR Biosciences Inc., Lincoln, NE) at Graswang and Fendt. All the measurement variables used in this study are given in Table 2.

Table 2 Measurement devices and meteorological parameters at the Fendt site

| Variable/parameter name | Unit | Measurement height | Instrument model |
|---|--------------------------------|------------------------------------|--------------------|
| Net radiation | W/m ² | 2 m | CNR4, Kipp & Zonen |
| Relative humidity | % | 2.2 m | WXT520, Vaisala |
| Air temperature | °C | 2.2 m | WXT520, Vaisala |
| Barometric pressure | hPa | 1.3 m | CS100, Setra |
| Wind speed | m/s | 2.2 m | WXT520, Vaisala |
| Wind direction | deg | 2.2 m | WXT520, Vaisala |
| Precipitation | mm | 2.2 m | Pluvio, Ott |
| Soil volumetric water content | m ³ /m ³ | 2-, 6-, 12-, 25-, 35-, 50-cm depth | CS616, Campbell |
| Soil temperature profile | °C | 2-, 6-, 12-, 25-, 35-, 50-cm depth | T107, Campbell |
| Soil heat flux plate | W/m ² | 8-, 9-cm depth | HFP01, Hukseflux |
| 3-D sonic anemometer | – | 3.5 m | CSAT3, Campbell |
| Open-path CO ₂ and H ₂ O gas analyzer | – | 3.5 m | LI7500, LI-COR |

2.4 Data coverage

Missing data in the measurements inevitably occurred. The gaps in the observed data make it difficult to estimate the annual latent heat (LE) and the sensible heat (H) fluxes and result in reduced quality of the data to validate model outputs (Hui et al. 2004). Some data were removed during the QC process by the TK3 software: This was done through two tests, i.e., *steady state test* (Gurjanov et al. 1984; Foken and Wichura 1996) and the *integral turbulence characteristics test* (Foken et al. 2004). According to Table 3, the overall quality flags are:

- I. flag 0: high quality data, which is used in fundamental research
- flag 1: moderate quality data, which have no restrictions to be used in the long-term observation programs, and
- II. flag 2: low data quality, which was removed.

For more details See Mauder et al. (2013).

Based on Table 4, the highest annual fraction of missing values for H (38%) and LE (44%) were observed at the Graswang site, whereas the lowest ones (H 13% and LE

20%) were found at the Rottenbuch site. Meanwhile, 27% of H and 33% of LE annual missing values were observed at the Fendt site. The main reason for this discrepancy could be explained, apart from the different landscape/environmental conditions at the sites, by the dissimilarity in the measurement instruments. In fact, enclosed-path and open-path systems are used in the Rottenbuch and Graswang sites, respectively. Enclosed-path gas analyzers, however, have a number of advantages, such as minimal data losses due to precipitation events, no surface heating problems, and the possibility of climate control. Therefore, with an enclosed-path gas analyzer installed at the Rottenbuch site, the highest (valid) data availability was observed during the examined period. Despite using the same gas analyzer (open-path system) at the Fendt and Graswang sites, a higher number of missing values were observed at the Graswang site. This could be explained by the weather/climate conditions. Compared to the other sites, Graswang is located in the southern part of the TERENO prealpine region and has more rainfall/snow days throughout the year. As a result, more measured data are invalid and should be removed. Correspondingly, the maximum number of seasonal missing values of the turbulent fluxes was found at Graswang (H -max: 51% and LE -max: 55%) in autumn 2013 and the minimum number for Rottenbuch (H -min: 6% and LE -min: 7%) in summer 2014. More detailed information regarding the missing values of the turbulent fluxes is given in Table 4.

Figure 2 shows the percentage of the diurnal and nocturnal missing values of the turbulent fluxes for each EC site. Obviously, the nighttime missing values were approximately more than twice the daytime values for all the sites. In addition, slightly more LE values were missing than those of H . This is because the LE measurement requires two fully functional instruments; a sonic anemometer plus gas analyzer, while H can be measured by the sonic anemometer alone, at least if the Schotanus correction is applied. Furthermore,

Table 3 Overall flag system after the Spoleto agreement, 2004 for CarboEurope-IP (Mauder and Foken 2015)

| Steady state (deviation in %) | Integral turbulence characteristics (deviation in %) | Final flags |
|-------------------------------|--|-------------|
| < 30 | < 30 | 0 |
| < 100 | < 100 | 1 |
| > 100 | > 100 | 2 |

Table 4 Percentage of the seasonal and annual missing values of the turbulent fluxes at the TERENO EC sites during 2013–2014

| Sites | Percentage of data gaps (%) | | | | | | | | | |
|------------|-----------------------------|------|--------|------|--------|------|--------|------|-----------|----|
| | Winter | | Spring | | Summer | | Autumn | | Annual | |
| | 2013 | 2014 | 2013 | 2014 | 2013 | 2014 | 2013 | 2014 | 2013/2014 | |
| Fendt | H | 27 | 20 | 22 | 34 | 26 | 25 | 34 | 31 | 27 |
| | LE | 40 | 22 | 28 | 40 | 37 | 30 | 38 | 35 | 33 |
| Graswang | H | 46 | 32 | 26 | 41 | 27 | 40 | 51 | 46 | 38 |
| | LE | 54 | 34 | 37 | 46 | 41 | 44 | 55 | 50 | 44 |
| Rottenbuch | H | 14 | 9 | 10 | 18 | 10 | 6 | 15 | 27 | 13 |
| | LE | 25 | 13 | 18 | 39 | 15 | 7 | 20 | 27 | 20 |

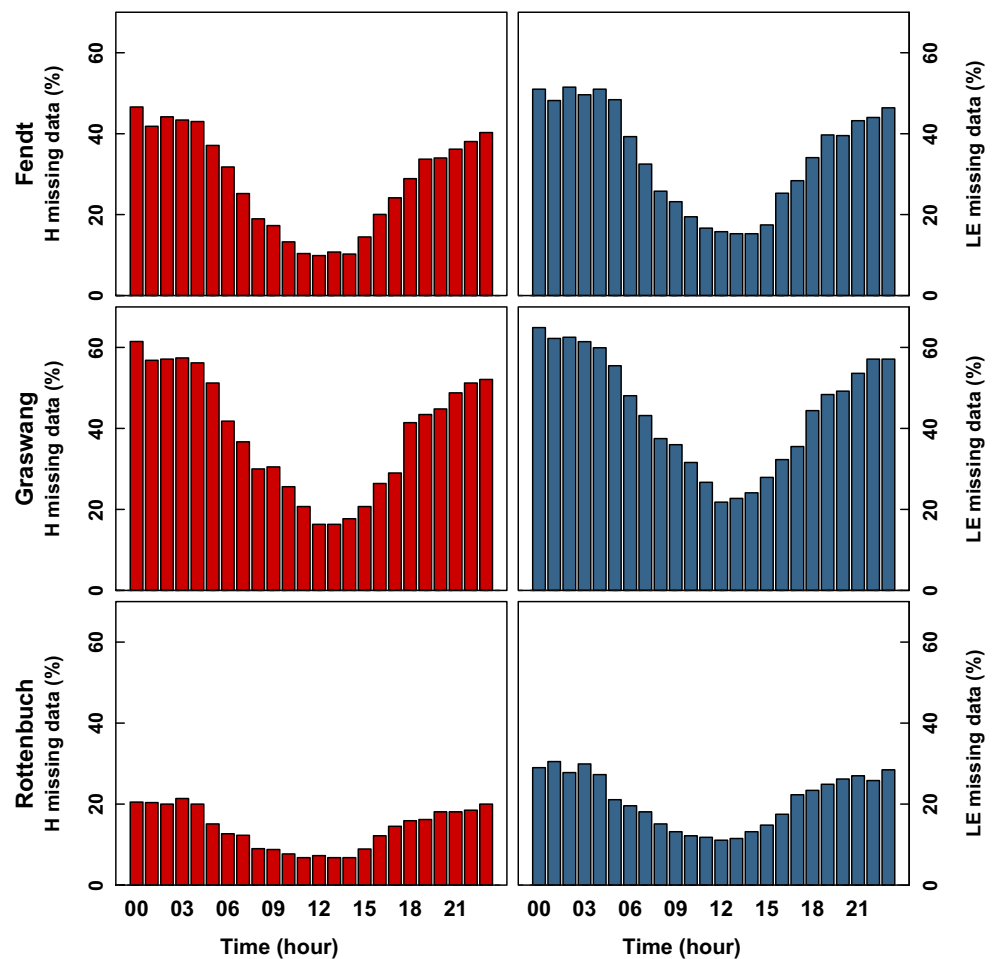
the Fendt and Graswang sites showed a similar pattern, i.e., distribution of missing values (due to using the same gas analyzer), meaning that the lowest diurnal and highest nocturnal missing values were found. The difference between diurnal and nocturnal missing values was much lower at the Rottenbuch than Fendt and Graswang. Moreover, this site had the lowest turbulent flux missing values (approximately three times less) compared to the other EC sites, due to an enclosed-path gas analyzer.

3 Results and discussion

3.1 Soil temperature and soil volumetric water content

The near-surface soil temperature and soil moisture are the key variables that control the exchange of water and heat energy between the land surface and the atmosphere (Wei 1995; Wang et al. 2010). The seasonal variations of daily mean of the net radiation (R_n), soil temperature (T_s), and soil

Fig. 2 The percentage of the diurnal and nocturnal missing values of the turbulent fluxes (H and LE) at the TERENO prealpine EC sites for the period of January 2013 to December 2014

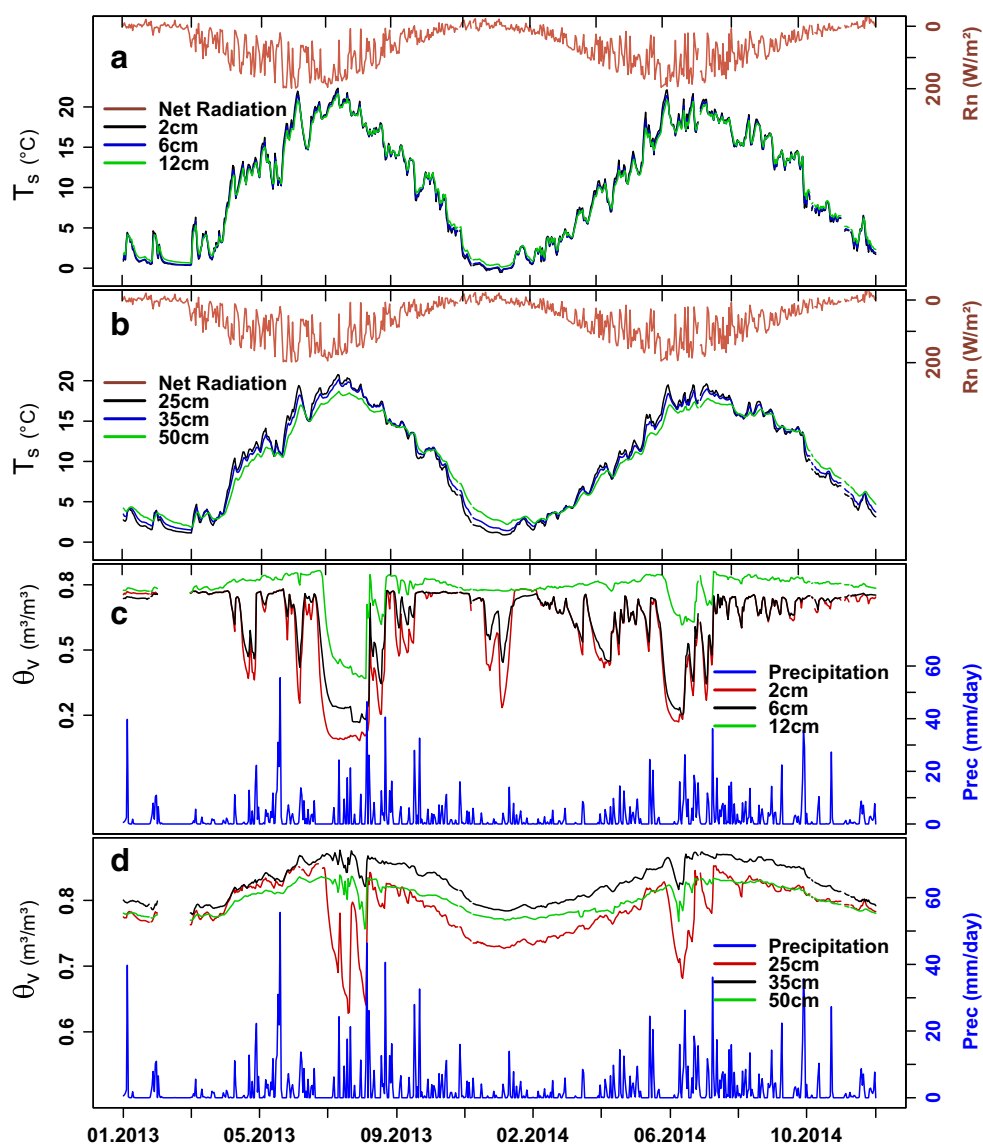


volumetric water content (θ_v) at depths of 2, 6, 12, 25, 35, and 50 cm and 24-h accumulated precipitation (Prec) at the Fendt EC site during 2013–2014 are shown in Fig. 3. The monthly mean 24-h R_n showed an obvious daily variation mainly because of the clouds. T_s in shallow layers of 2-, 6-, and 12-cm showed little difference in each season. It is not surprising that mean daily T_s at topsoil does not drop below the zero degree due to the snow cover during the wintertime. The differences in seasonal T_s between the deep layers at 25, 35, and 50 cm were larger than those of measured in the layers close to surface at 2, 6, and 12 cm. This otherwise unusual finding can be explained by a change in soil texture from 35 to 50 cm towards much higher clay content. The maximum T_s was measured in July 2013 (Fig. 3a and b). As indicated in Fig. 3c and d, the topsoil was highly saturated ($> 0.7 \text{ m}^3/\text{m}^3$) with the water content during the winter and autumn seasons and only reduced to approximately $0.3 \text{ m}^3/\text{m}^3$ during the winter 2014.

Whereas in the deep layers, the maximum and minimum values of θ_v can be found during the summer and winter seasons, respectively. In the summertime, despite the fact that there was a considerable amount of rainfall, the θ_v periodically decreased dramatically, mainly at the layers near to the surface. This can be explained by the following: Fendt as a grassland site, located at the bottom of a shallow valley with a low gradient, and the groundwater and surface-water interactions can be an important mechanism in the region. Thus, the most probable reason for the sudden θ_v changes might be related to changes in the groundwater level for that site.

Although no groundwater level measurements were available for our study period 2013–2014, the findings obtained by Wolf et al. (2017) for the ScaleX-2015 campaign at the Fendt site confirmed that interactions between the groundwater level and surface-water exist. After strong rainfall events, the infiltration or drainage of excess water is the dominant runoff, and

Fig. 3 Daily mean variations. **a–b** Soil temperature (T_s) at depths of 2, 6, 12, 25, 35, and 50 cm and net radiation (R_n). **c–d** Soil moisture (θ_v) at depths of 2, 6, 12, 25, 35, and 50 cm and precipitation (Prec) at the Fendt EC site for the period of January 2013 to December 2014. The data are averages of 24-h values



during the recession of stream flow, the contribution of groundwater to runoff is increased. They also conclude that the full mechanisms for the interactions of runoff generation and storage system for that area have not been fully investigated. In addition to the high influence of the groundwater level on the soil moisture in the region, other factors might be considered, such as unequally distributed summertime rainfall events, high evapotranspiration rate due to the high temperature, and runoff generation. Therefore, for the above reasons, the amount of θ_v in some short periods was quite low, especially during the summertime.

3.2 Energy partitioning

The average contribution of the turbulent fluxes to the surface energy budget was calculated for each season (Table 5). The average seasonal values of H/Rn in spring, summer, autumn, and winter was calculated as 0.12, 0.11, 0.34, and 0.64; while LE/Rn values were 0.53, 0.58, 0.50, and -0.20 , respectively at the Fendt EC site. Meanwhile at the Rottenbuch site, the corresponding H/Rn values were calculated as 0.14, 0.11, 0.37, and -0.30 and also LE/Rn values measured as 0.37, 0.51, 0.18, and 0.11, respectively. The seasonal value of H/Rn in the autumn and spring seasons at the Graswang EC site was measured as -0.09 and -0.006 , respectively, which were quite low and close to zero. This was because of the snow cover, which caused the land surface to be cold and as a result, a negative sensible heat flux (downwards) occurred during that period.

Furthermore, the seasonal noontime variations of the Bowen ratio indicated high seasonal variations throughout the year at the EC sites. In winter, 86.0, 90.4, and 65.7 and in autumn 89.3, 92.4, and 78.5 of heat was transferred (either positive/upwards or negative/downwards) as LE flux at the Fendt, Rottenbuch, and Graswang EC sites, respectively. Meanwhile, the corresponding values during the spring and summer were 98.5, 99.6, and 83.4 and 99.8, 99.3, and 96.7%, respectively at the aforementioned EC sites. The Bowen ratio values in warm periods (spring and summer) were mostly positive with low magnitudes due to the high contribution of LE , while during the cold seasons (winter and autumn), the ratio was negative because of negative H values over those periods (figures not shown).

3.3 Turbulent flux variability on different time scales

3.3.1 Management of grassland at the EC sites

The management of grassland is quite different between the southern and northern parts of the TERENO prealpine region (Fig. 4), which indicates an elevation trend for that area. At the highest elevation site, i.e., Graswang (860 m), one or two grass cuts are done per year usually starting from the early

June to mid-August, which indicates that the grass cutting is exclusively limited to months with the highest temperatures. Meanwhile, at the middle and low elevation sites, i.e., Rottenbuch (770 m) and Fendt (598 m), respectively, the farmers begin to cut the grass from mid-May to late October, leading to four to five cut times. The last grass cuts of the year are done almost simultaneously at these sites. Furthermore, a coincidence between the grass cutting events and a sudden decrease of albedo after the grass cutting was sometimes observed. A sudden drop of the albedo at the beginning of August 2014 at the Fendt EC site can demonstrate this effect.

The mean daily based variation of surface albedo, which is highly influenced by the snow cover, soil color and moisture, vegetation cover, etc., at the study sites is shown in Fig. 4, as well. Overall, the highest albedo values were measured during the winter and autumn seasons, whereas the lowest ones observed during the summer and spring periods mainly due to the snow cover in cold periods and rather high soil moisture, as well as high vegetation fraction in the warm periods throughout the year. The maximum surface albedo was measured during January and April 2013 due to the high snow cover at the EC sites. The higher albedo values at the Graswang site (in the southern part) suggest an increase of snow cover in both height and duration for that area, which is also confirmed by the higher values of the outgoing short-wave radiation (OSR) at the higher elevated sites for the same times. Therefore, the radiative fluxes of OSR and albedo are highly affected by the grass cut events, which consequently influence the turbulent flux variability at the grassland EC sites in the region.

3.3.2 Drivers of the turbulent fluxes: PCA-based analysis

To determine the most relevant driving variables that influence the turbulent fluxes at the study sites, a PCA was applied. To enable comparability of the impact of the different

Table 5 Energy partitioning for individual seasons at the TERENO EC sites during 2013–2014. H/Rn and LE/Rn are the ratios of the turbulent fluxes to Rn and B is the Bowen ratio ($B = H/LE$)

| Sites | | Spring | Summer | Autumn | Winter |
|------------|---------|--------|--------|---------|----------|
| Fendt | H/Rn | 0.12 | 0.11 | 0.34 | 0.64 |
| | LE/Rn | 0.53 | 0.58 | 0.50 | -0.20 |
| | B | 0.23 | 0.20 | -0.29 | -0.30 |
| Rottenbuch | H/Rn | 0.14 | 0.11 | 0.37 | 0.37 |
| | LE/Rn | 0.37 | 0.51 | 0.18 | 0.11 |
| | B | 0.43 | 0.23 | -1.42 | 2.26 |
| Graswang | H/Rn | 0.15 | 0.13 | -0.09 | -0.006 |
| | LE/Rn | 0.62 | 0.60 | 0.34 | 0.24 |
| | B | 0.27 | 0.21 | -0.57 | -6.02 |

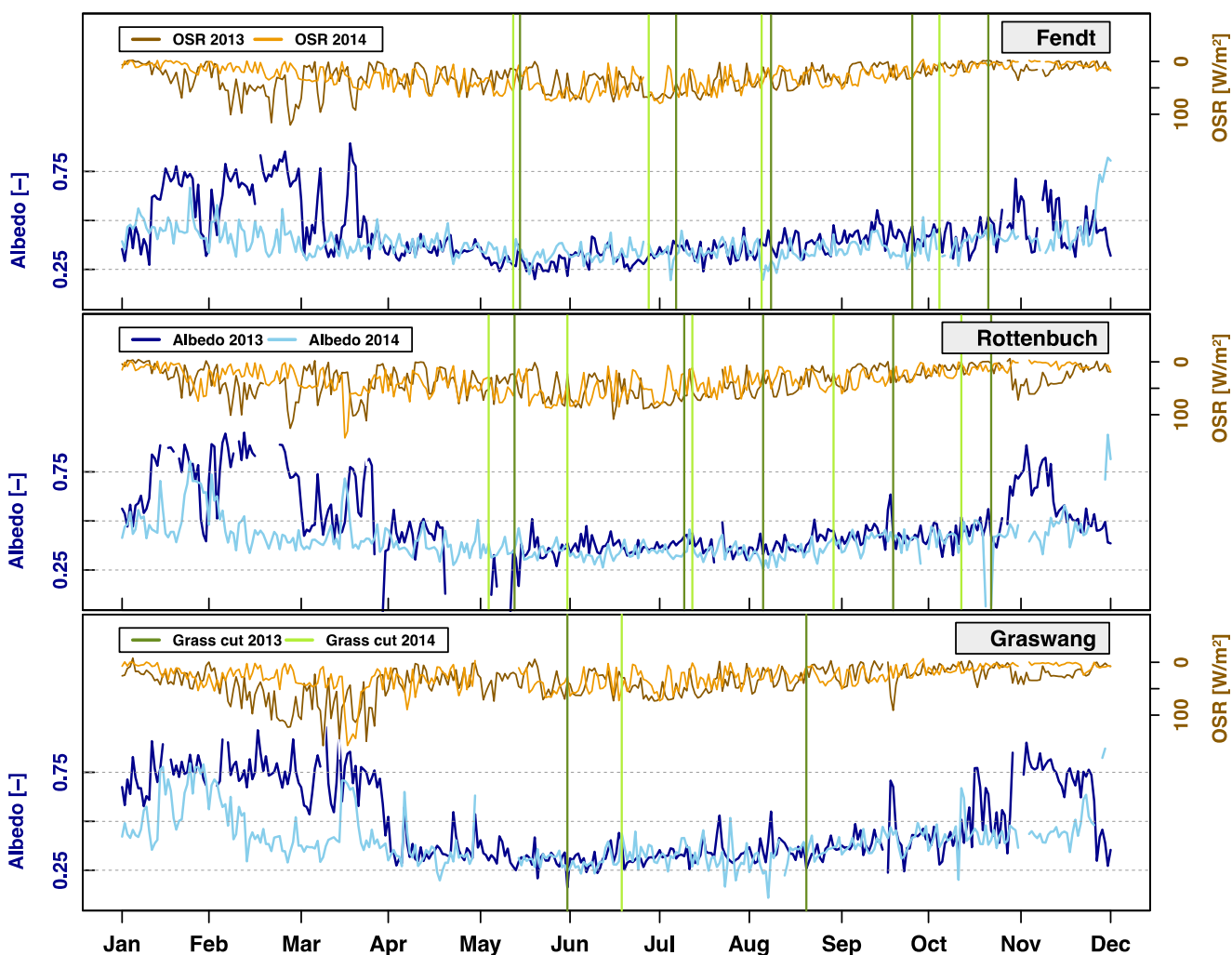


Fig. 4 Daily mean variations of the outgoing shortwave radiation (*OSR*) and albedo values, as well as the number of grass cuts at the TERENO prealpine EC sites for the period of January 2013 to December 2014

variables, the data are centered and scaled before application of the PCA. For the sake of visualization, the focus is on the first two PCs (PC1 and PC2), which explain >60% of the total variance of the original datasets (Fig. 5). The figure illustrates the cross-correlation and the contribution of each variable to the PCs at the different TERENO prealpine sites. The length (angle) of the arrows represents the magnitude (direction) of the correlation coefficient between the variable and the PCs, which the color of arrows indicates the contributions (importance) of the variables to the turbulent fluxes (12 variables ranked from blue (low importance) to red (high importance)). For Fendt, PC1 shows high positive correlations with the radiation components of net radiation: R_n ($r = 0.93$) and photosynthetic photon flux density: PPF ($r = 0.91$) with a total contribution of approx. 28.5% (not shown), as well as with the temperature variables of infrared surface temperature: SurfaceT ($r = 0.92$), air temperature: AirT ($r = 0.91$), and soil temperature at 2 cm depth: SoilT ($r = 0.89$) accounting for approximately 42.2% of the total contribution (not shown).

The variables of albedo ($r = -0.63$), soil moisture at 2-cm depth: SoilM ($r = -0.57$), and relative humidity: RH ($r = -0.56$) are negatively correlated with PC1. Furthermore, PC1 shows the highest correlation with R_n , which identifies net radiation as a key variable for the turbulent flux measurement at the Fendt EC site.

The aforementioned variables also represent approximately the same contributions and correlations to PC1 at the Rottenbuch EC site, except for the wind components of wind direction: WindD ($r = -0.47$) and wind speed: WindS ($r = -0.41$), which show no correlation with PC1 at the Fendt site. Their influence at the Graswang site, however, is lower, representing a rather different pattern compared to the other EC sites, except for the SoilT close to the surface ($r = 0.93$) with the highest contribution of 16% (not shown) and albedo ($r = -0.72$). Thus, the albedo rather follows an elevation trend in the TERENO region. This finding is in agreement with Zeeman et al. (2017) and might be explained by the lack of irradiation due to a mountain shadowing effect.

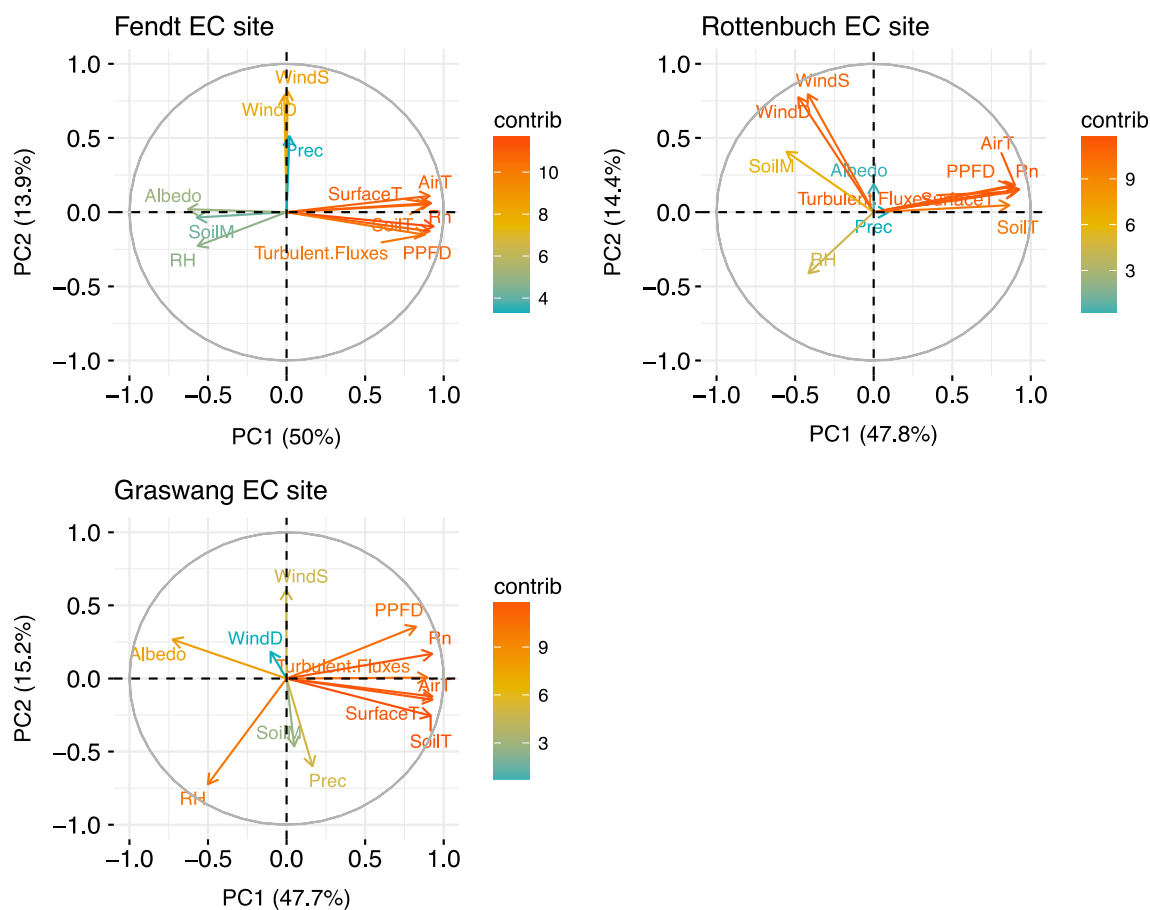


Fig. 5 Contribution of the meteorological variables to the turbulent fluxes (sum of H and LE) using a multivariate PCA analysis at the TERENO prealpine EC sites for the period from January 2013 to December 2014. Daily mean meteorological data include wind direction (WindD ($^{\circ}$)), wind speed (WindS (m/s)), air temperature (AirT ($^{\circ}$ C)), relative humidity (RH (%)), precipitation (Prec (mm)), soil temperature at 2-cm depth (SoilT ($^{\circ}$ C)), soil moisture at 2-cm depth (SoilM (m^3/m^3)),

photosynthetic photon flux density (PPFD ($\mu\text{mol}/(m^2 \text{ s})$)), albedo [–], net radiation (R_n (W/m^2)), and infrared surface temperature (SurfaceT ($^{\circ}$ C)). The length (angle) of the *arrows* represents the magnitude (direction) of the correlation coefficient between the variable and the PCs. The lowest and highest contributions of the variables to the turbulent fluxes are ranked with *colors* ranging from *blue* to *red*, respectively

The Graswang site possesses a mountain climate with high amounts of precipitation and snow events frequently occurring between October and April.

PC2 is highly correlated only with the WindS ($r = 0.81$ at Fendt, $r = 0.79$ at Rottenbuch, and $r = 0.60$ at Graswang) with a mean total contribution of 50% (not shown) and WindD (in order of aforesaid sites: $r = 0.78$, $r = 0.77$, and $r = 0.18$), accounting for approximately 35% (not shown) of the mean total contribution. PC2 lacks correlation with radiation and temperature components (<5%, not shown). Meanwhile, the contribution of WindS (20%, not shown) was much more than WindD (2.5%, not shown) at Graswang. This is because the site is located in a valley surrounded by high mountains and in such a way that the prevailing wind directions are easterly and westerly (See Fig. 1). This component represents the importance of the wind variables to the turbulent flux measurements in the region. Increased wind speed, for instance, also leads to an increase of the turbulence intensity and mixing, thereby increasing the fluxes. With respect to the precipitation: Prec

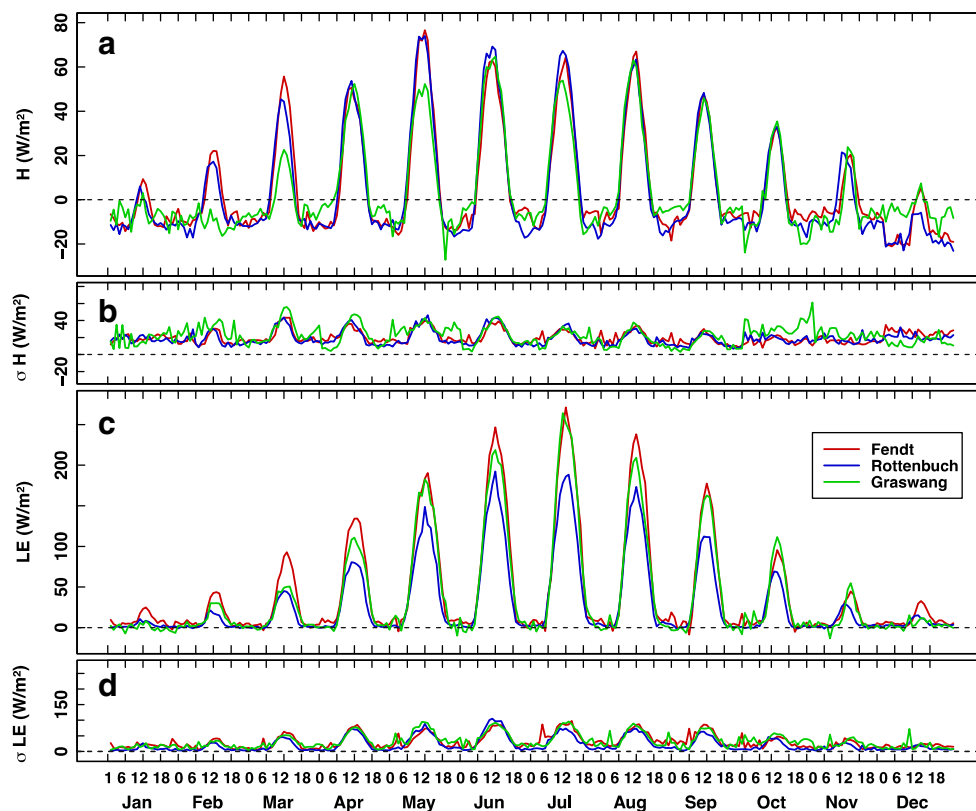
and RH variables, they are ranked as the second and third most important variables that are negatively correlated with PC2. Therefore, Prec holds the highest correlation ($r = -0.60$) at the Graswang site.

Overall, the PCA results found at the TERENO prealpine EC sites were consistent with findings of other studies over different ecosystems (e.g., Schmidt et al. 2011).

3.3.3 Monthly and seasonal variations of the turbulent fluxes

To understand the monthly mean diurnal turbulent fluxes at the study sites, their hourly variations together with the standard deviations (σ) are shown in Fig. 6. As expected, the variations of H and LE fluxes were low during the winter and autumn periods, whereas they were quite large during the spring and summer seasons in the region. During the cold periods, in winter for example, the peak values were 55.6 and 92.7 W/m^2 for H and LE fluxes observed at the Fendt site, respectively. The mean diurnal values of H at the Graswang

Fig. 6 Monthly mean diurnal variation and standard deviation (σ) of the sensible heat flux (H) and the latent heat flux (LE) at the TERENO prealpine EC sites for the period of January 2013 to December 2014. The data represent hourly averages



site were quite different from the other two sites as a result of different landscapes and topography.

In February, for example, the highest measured H was -1.55 W/m^2 due to a very cold surface in that area. Thus, the highest and lowest monthly σ values of H were found at the Graswang as 55.7 and 6.2 W/m^2 , respectively (Fig. 6b). The differences between day and night H and LE values were not very pronounced in the wintertime because of the low radiation variation in the study area. For the warm periods, the mean diurnal values of H and LE fluxes showed much larger differences due to the increase of solar radiation, precipitation events, as well as the high vegetation fraction over the experimental period, and obviously, the main consumer of R_n was LE at the sites.

The lowest mean monthly LE flux in Rottenbuch can be explained by the different soil textures at that site, which is mostly sandy loam at the surface, as well as a gravel layer at about 50-cm depth (and continues to deeper layers). This causes precipitation to infiltrate quickly into the deep ground and thus the surface dries out rapidly soon after rainfall events. Moreover, the lowest mean monthly H flux occurred shortly after noon at Graswang, which might be explained by the shading condition in that area, meaning that the sun sets rather early as the site is surrounded by high mountains. The highest LE fluxes occurred in July as the highest amount of precipitation takes place during the summertime. The magnitude of variations increased from winter to summer and accordingly

showed a decrease from summer to winter corresponding to the variation of radiation, precipitation patterns, soil moisture/types, and different landscapes across the TERENO prealpine region.

Seasonally, all the energy fluxes of R_n , H , LE , and G at the Fendt EC site showed distinct diurnal cycles over the experimental time (Fig. 7). R_n was highly variable between cold and warm seasons and also, the range of the daytime cycle of R_n increased from autumn to summer and decreased vice versa. Thus, the variation of the diurnal cycle of R_n was strong during summer but weak during autumn (Fig. 7a). The range of H values increased from autumn to spring. The nocturnal H value was significantly negative, meaning that the heat was transferred from the atmosphere to the land surface due to the cold surface. The seasonal variation of H was rather small compared to R_n , which was quite large between the cold and warm periods. LE flux had an obvious seasonal diurnal variation during summer with the value of 245.1 W/m^2 , which became rather small in spring (179.1 W/m^2) and then remarkably decreased during the autumn (58.3 W/m^2) and winter (50.6 W/m^2) seasons (Fig. 7e). Finally, the G flux had a rather similar and less seasonal variation throughout the year. The nocturnal G value was significantly negative (upwards) compared to other energy fluxes. Interestingly, the maximum diurnal G flux (25.1 W/m^2) in winter occurred at 13:00 pm, which indicated a shift of around 1 h. This might be explained by the snow cover in the region causing a short delay for the heat to

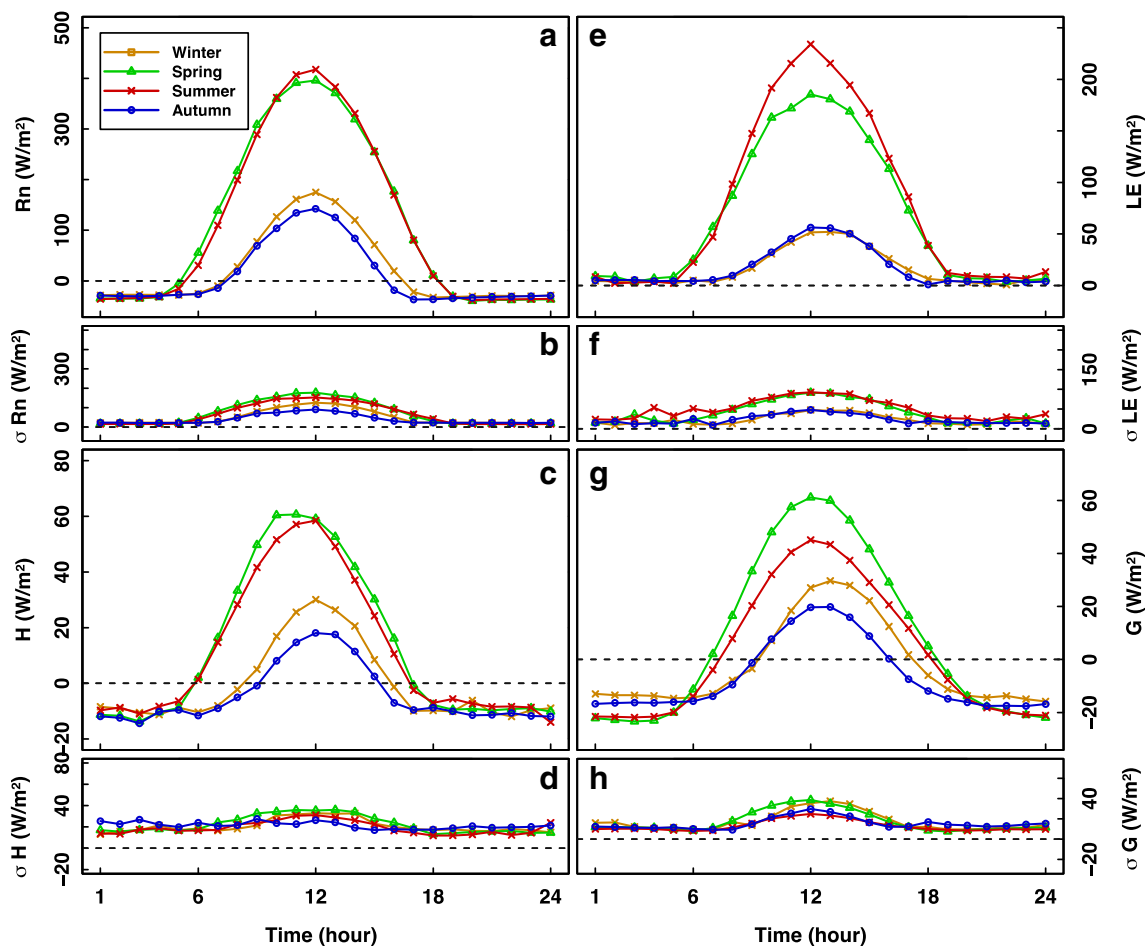


Fig. 7 Diurnal cycle of seasonal mean variations and standard deviation (σ) of the surface energy fluxes at the Fendt EC site for the period of January 2013 to December 2014. The data represent hourly averages

be diffused in the soil (Fig. 7g). Overall, the highest seasonal diurnal variations were observed in Rn , followed by LE , H , and G .

3.4 Energy balance closure

3.4.1 Overall and seasonal energy balance closure

The linear regressions between the turbulent fluxes and the available energy at the TERENO prealpine EC sites of Fendt, Rottenbuch, and Graswang are shown in Fig. 8. The EBC is defined as the slope of a regression analysis of turbulent energy transport against available energy, forced through zero. The EBC values were 0.65, 0.56, and 0.65 and the coefficients of determination (R^2) values were 0.82, 0.85, and 0.77 at the Fendt, Rottenbuch, and Graswang sites, respectively. The lowest R^2 between measured and available energy was found at the Graswang site. This can be explained by the climatic and environmental conditions. This site is surrounded by high mountains (See Fig. 1) and the wind speed is relatively low so that the mechanically driven turbulence is reduced in the valley. As a result, many of the calculated H and LE values were removed

as unreliable data during the post-processing (i.e., QC) by the TK3 software. Thus, the Graswang site had the lowest number of data ($n = 7969$) compared to other EC sites (Fig. 8c). In terms of EBR, as defined in Eq. 3, the highest overall value of EBR (0.73) was calculated at the Graswang site indicating that the minimum heat and water vapor fluxes are lost for that area, which is due to the geographical location of the site. Furthermore, the lowest slope (0.56) and EBR (0.56) values were found at the Rottenbuch site. A spectral analysis (not shown) indicated that this underestimation of the turbulent fluxes calculated at the Rottenbuch site was not due to the frequency response corrections, e.g., through tube attenuation. Therefore, this finding is partially explained by the heterogeneity of the land surface type around this site, meaning that the site itself is located closely to a town, which has a much higher temperature than the meadow and there is a deep canyon of the Ammer river nearby, which has a lower temperature. Thus, it is likely that the advection of heat and vapor had occurred in that area (Fig. 8b). Furthermore, the research done by Eder et al. (2014) shows that there is a relationship between landscape-scale heterogeneity and EBC for the TERENO prealpine sites. The mean EBR was 0.65 for the TERENO prealpine region.

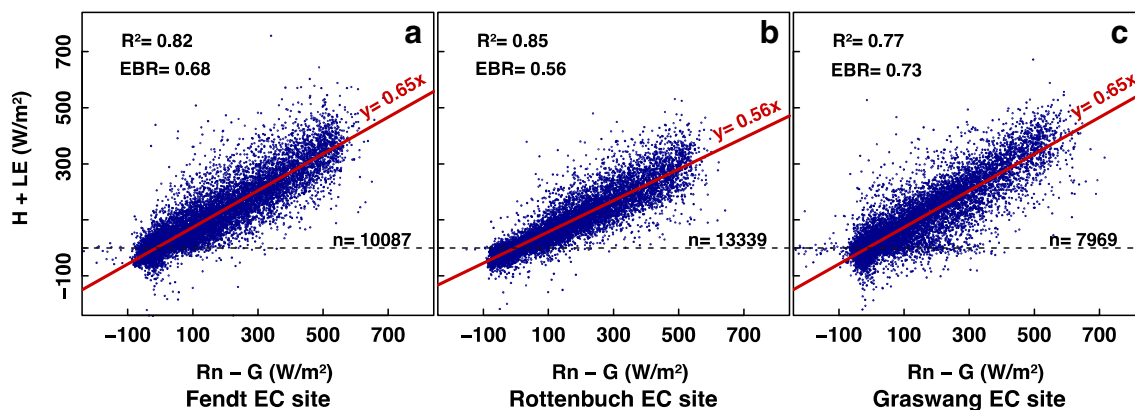


Fig. 8 Intercomparison of the turbulent fluxes ($H + LE$) against the available energy ($Rn - G$) at the TERENO prealpine EC sites for the period of January 2013 to December 2014. The gray horizontal dashed line indicates the zero value. The data represent half-hourly averages

The seasonal differences between the values of EBR at the TERENO EC sites are given in Table 6. The highest seasonal EBR values were 0.70 in summer and 0.81 in autumn, while the lowest corresponding values were 0.42 and 0.61 in winter at the Fendt and Graswang sites, respectively. The lowest seasonal EBR values were calculated as 0.51, 0.65, 0.47, and 0.33 in spring, summer, autumn, and winter, respectively at the Rottenbuch site. Overall, warm seasons showed a higher EBR value compared to the cold ones at the study sites, except for the Rottenbuch site in which a considerable seasonal difference could not be found.

3.4.2 Seasonal energy balance residual

The seasonal mean of diurnal variation of the energy balance residual (Res) is shown in Fig. 9. The largest maxima of the Res were 140.8 W/m^2 in spring, 90.1 W/m^2 in summer, and 141.9 W/m^2 in summer at Fendt, Graswang, and Rottenbuch sites, respectively. The Rottenbuch site had the highest Res in warm periods owing to the heterogeneity of the landscape in that area. The autumn diurnal Res sharply decreased from 40.5 to $-30.9 W/m^2$ in the afternoon at the Graswang site. This might be explained by the lack of sunshine in the afternoon, as this tower is surrounded by high mountains (See Fig. 1 for the location) and the sun accordingly sets earlier due to the elevated horizon.

Overall, the reasons for obtaining poor EBC may result from either measurement or method limitations. Some of these

effects include (a) net radiation sensors, which might perform poorly in the field; (b) wind speed and temperature measurements, e.g., vertical wind speed underestimation; (c) water vapor fluctuation measurements, e.g., inappropriate performance of sonic anemometer during and after rainfall events; and (d) the soil heat flux and heat storage measurements (Culf et al. 2004). In all parts of the world, researchers have encountered energy residuals of magnitudes similar to our datasets (e.g., Foken and Oncley 1995; Panin et al. 1996; Wicke and Bernhofer 1996; Foken et al. 1999; Kahan et al. 2006; Oncley et al. 2007; Su et al. 2008; Wang et al. 2010). The study of Eder et al. (2014) on the EBC suggests that part of the imbalances might be explained by the mesoscale transport in relation to the heterogeneity of the landscape, which has been hypothesized for other sites by Mauder et al. (2007) and Panin and Bernhofer (2008), as well. Therefore, to quantify the possible reasons for the lack of energy balance at the TERENO EC sites, the diurnal and nocturnal variations of the heat fluxes, influence of the time of day, as well as the effect of flux measurement footprint and the dependence of the EBC on the wind direction are analyzed in the following subsections.

3.4.3 Influence of the diurnal and nocturnal conditions

Figure 10 shows the daytime and nighttime correlations of the turbulent fluxes vs. the available energy. The daytime and nighttime R^2 were 0.73 and 0.093, respectively, at the Fendt site. The highest/lowest daytime and nighttime R^2 were calculated as 0.79 and 0.70 and 0.22 and 0.026 at the Rottenbuch and Graswang sites, respectively. Furthermore, the Graswang site had the lowest diurnal and nocturnal data availability (i.e., N 6511 and N 2013, respectively), while the highest corresponding valid values were N 8046 and N 5785 that were observed at the Rottenbuch site. Other researchers have reported a better diurnal EBC (e.g., Wilson et al. 2002). The large nighttime energy imbalances could be explained by weak turbulence at night. Aubinet et al. (1999) and Blanken et al. (1997) also came to the conclusion that when the friction

Table 6 Seasonal EBR at the TERENO EC sites during 2013–2014

| | Site | Season | | | |
|---------------------------------------|------------|--------|--------|--------|--------|
| | | Spring | Summer | Autumn | Winter |
| $EBR = \frac{\sum(LE+H)}{\sum(Rn-G)}$ | Fendt | 0.68 | 0.70 | 0.69 | 0.42 |
| | Rottenbuch | 0.51 | 0.65 | 0.47 | 0.33 |
| | Graswang | 0.76 | 0.73 | 0.81 | 0.61 |

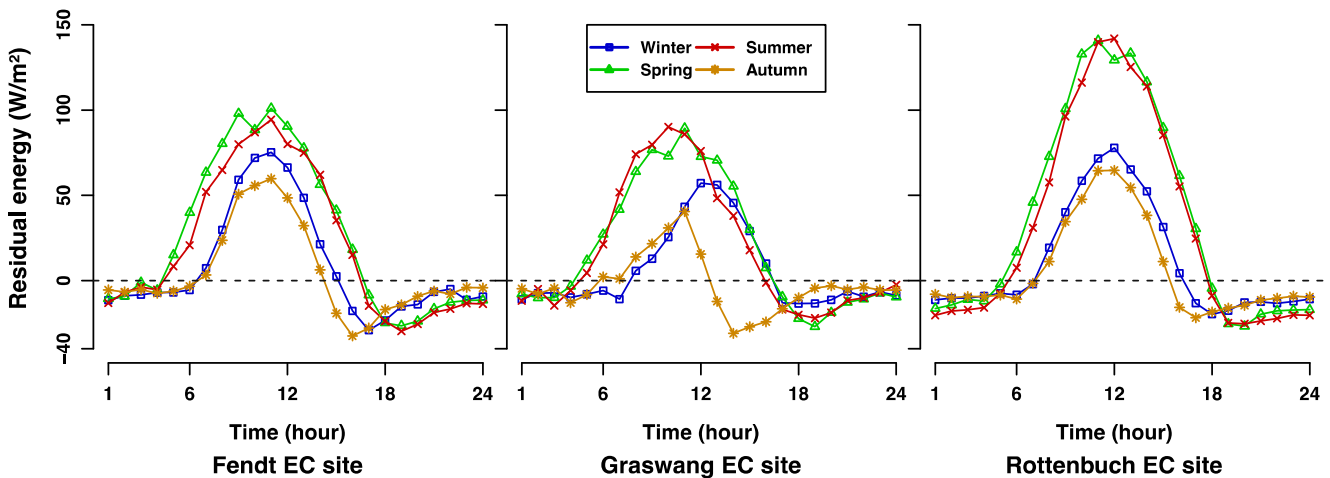


Fig. 9 Seasonal 24-h cycle of the residual energy ($Res = Rn - (H + LE + G)$) at the TERENO prealpine EC sites for the period of January 2013 to December 2014. The data represent half-hourly averages

velocity is small, the energy imbalance is usually high during the nocturnal periods. Lee and Hu (2002) found that a low energy balance during nighttime periods was due to mean vertical advection, as well.

3.4.4 Dependence on the time of day

The diurnal courses of the EBR and the energy balance residual, as well as with the mean magnitudes of the measured and available energy are shown in Fig. 11. We found that for our sites the

EBR is not meaningful from 1:00 to 6:00 UTC and after 17:00 UTC, when the available energy was close to zero. Between these two periods, however, a linear increase in the EBR (with a different pattern and intensity) was observed at the EC sites. At all three EC sites, a sharp increase in the EBR was observed after 15:00 UTC, indicating a better EBC or even over-closure in the afternoon. Such an observation normally points to an unaccounted storage term, which is filled in the morning and depleted in the afternoon. Since we have included any soil heat storage in G , only the heat stored in the biomass can explain our

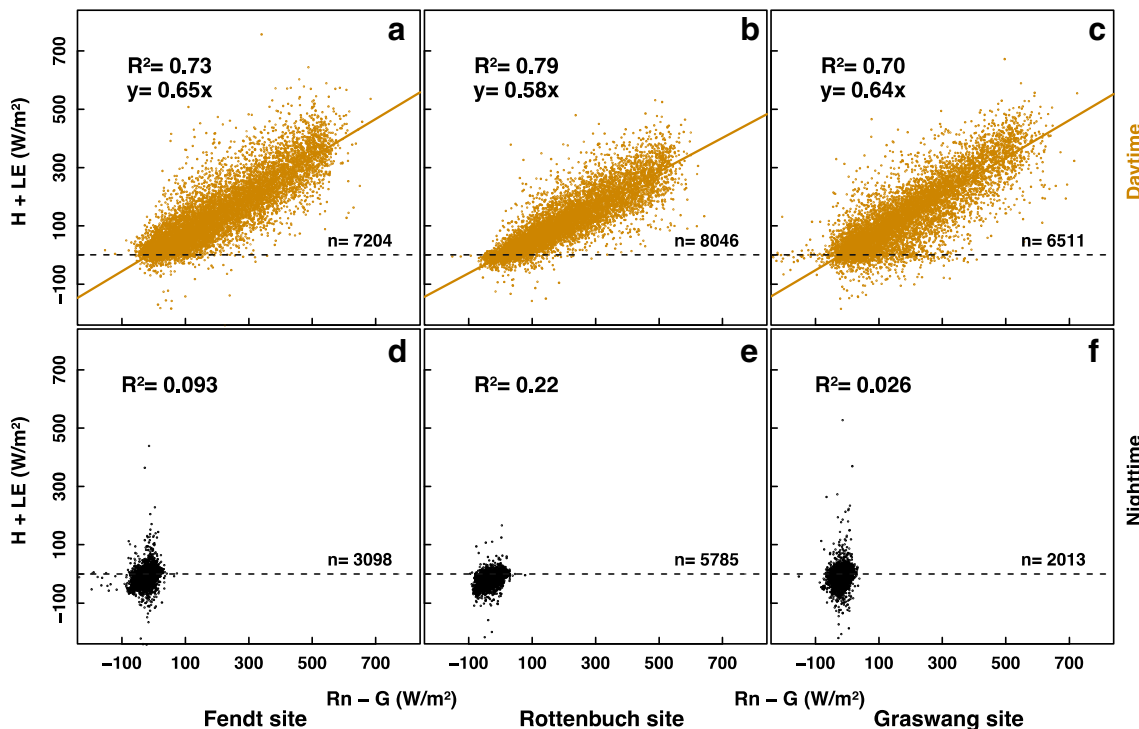


Fig. 10 Turbulent fluxes ($H + LE$) vs. available energy ($Rn - G$) for daytime and nighttime at the TERENO prealpine EC sites for the period from January 2013 to December 2014. The data represent half-

hourly averages. The daytime hours was defined as the incoming shortwave radiation ($ISR > 25 \text{ W/m}^2$)

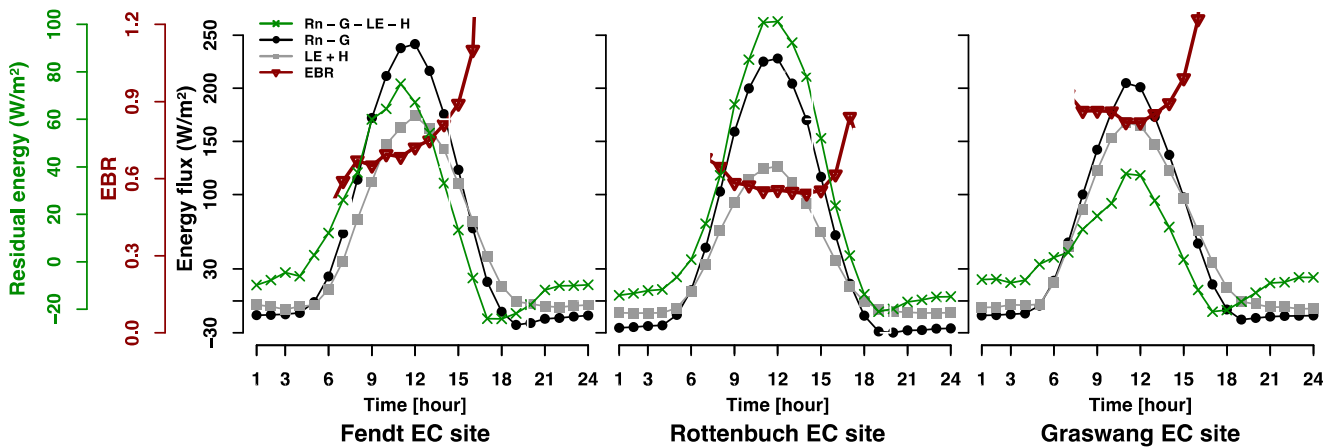


Fig. 11 The mean diurnal variation of: the available energy ($Rn - G$), the turbulent fluxes ($LE + H$), the energy balance ratio (EBR), and the residual energy ($Rn - G - LE - H$) at the TERENO prealpine EC sites for the period of January 2013 to December 2014

finding. Thus, the best closure occurred in the afternoon, peaking shortly before the sunset (at approximately 18:00) at all the EC sites. Besides, the residual energy exhibited an almost similar diurnal pattern but different in magnitude from the study sites, which is characterized by positive values from approximately 4:00 to 15:00 and by negative values outside this time period ranging from 100 W/m^2 at the Rottenbuch site to $-24 W/m^2$ at the Fendt site, where the EBC peak occurred.

3.4.5 Effect of the flux footprint

The turbulent vertical flux of a passive scalar measured up-wind of the surface area represents the exchange between the

atmosphere and the surface over a larger area is known as the atmospheric flux footprint or footprint (Horst 1999; Sanchez et al. 2010). An increase in the measurement height and decrease in the surface roughness, as well as changing the atmospheric stability from unstable to stable would lead to an increase in size of the footprint and move the peak contribution away from the EC site. These are the main factors affecting the size and shape of the flux footprint. The overall flux footprint climatologies at the TERENO prealpine EC sites are shown in Figs. 12, 13, and 14. The aerial Google Earth images in the region clearly show the heterogeneous surface at the EC sites in which a stronger directional surface inhomogeneity is observed at the Rottenbuch site (Fig. 13) as the site is situated

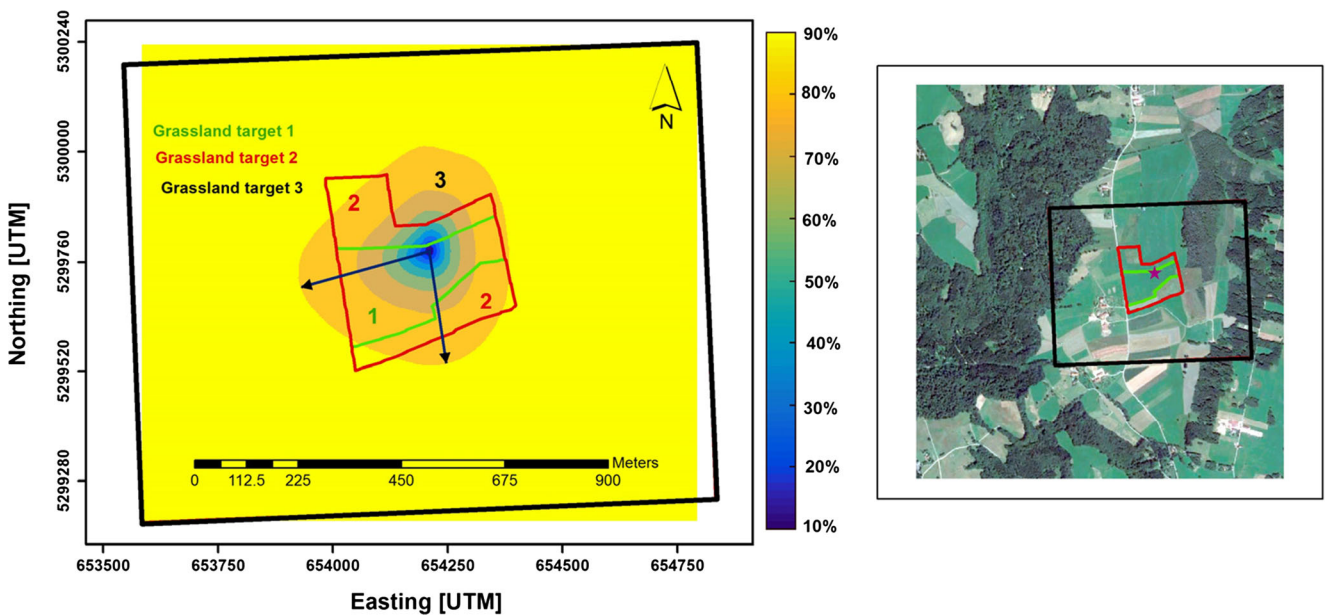


Fig. 12 Footprint climatology of the Fendt EC site. The *left side map*: background filled contours indicate the cumulative percentages of the annual mean half-hourly flux footprint during 2013–2014, and the *overlaid colorful domains* represent the different grassland targets, where the canopy height differs at the targets. The *dark blue arrows*

show the most dominant footprint directions. The *right side map*: the domains overlaid on the Google Earth image indicate the approximate position of the grassland targets surrounding the site. See Fig. 1 for further map details

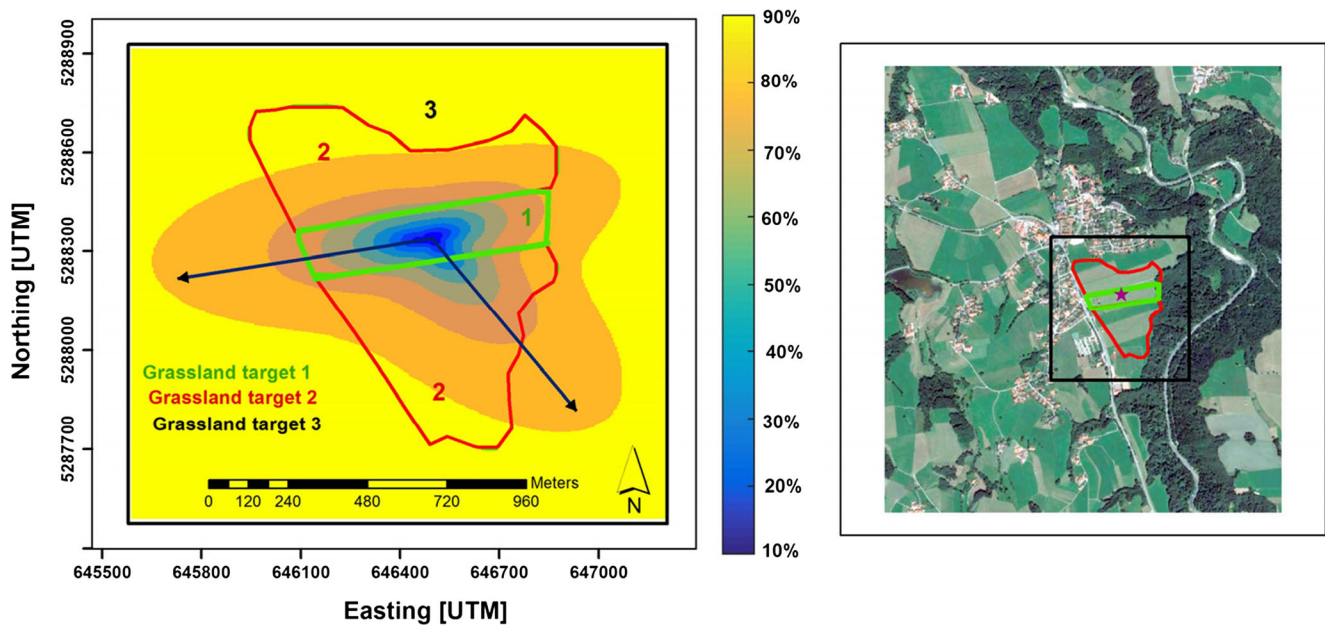


Fig. 13 Same as in Fig. 12 but for the Rottenbuch EC site

close to a town, as well as a deep canyon (i.e., Ammer river). Figure 12 shows that approximately 80% of the turbulent flux contribution is received by the Fendt EC site instruments from the grassland targets 1 (~60%) and 2 (~20%) located in a radius of approximately 220 m from the station and less than 10% of the flux contribution is emitted by target 3, which is farther away from the instruments. In addition, the overall shape of the flux footprint strongly matches the direction of the prevailing wind for that area (See Fig. 1 for the details).

As shown in Fig. 13, instruments of the Rottenbuch EC site receive more than 65% of the annual flux footprint contribution from the grassland target 1 and approximately 25% from

the grassland target 2. Thus, the fetch is larger compared to other EC sites.

As mentioned earlier, the lowest EBR at the Rottenbuch site could be explained by the combined effects of the presence of the Ammer river located about 600 m east-southeast of the station and the nearby town situated west-north of the EC site. Both these factors are a source of small-scale heterogeneity (Schmid 1997; Eder et al. 2014). The size of the flux footprint also confirms this mismatch, where some percentage of the footprint is emitted from those inhomogeneous areas. The grassland targets 1 and 2 emitted approximately 90% of the flux footprint concentration at the Graswang EC site (Fig.

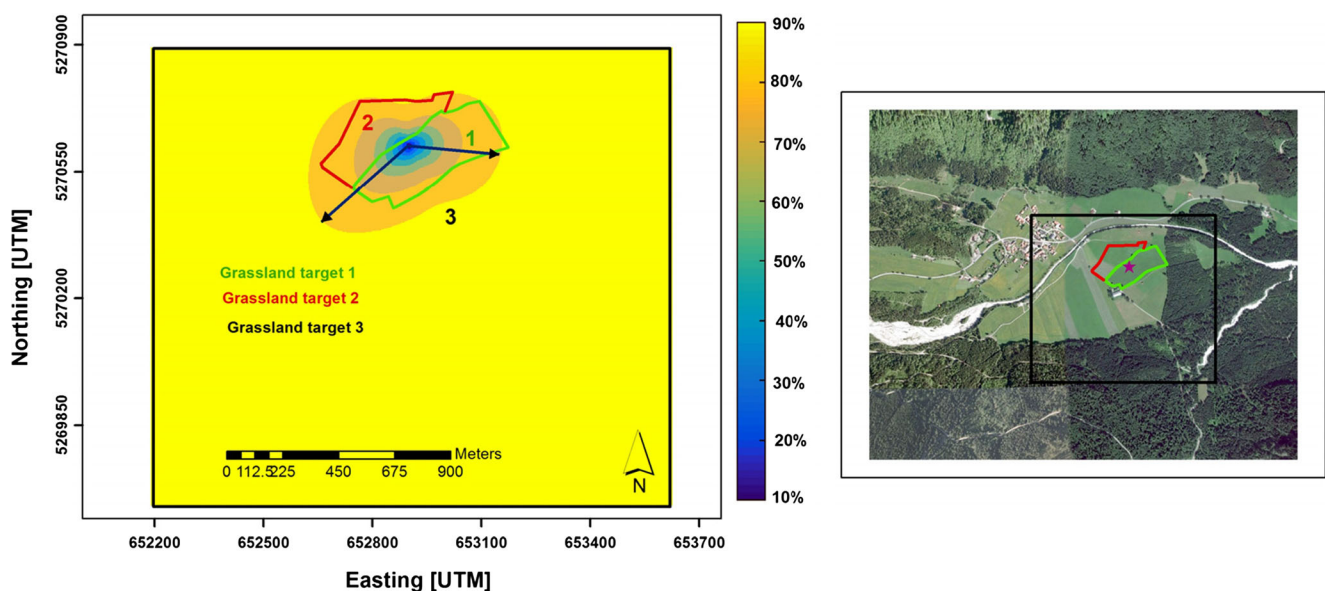


Fig. 14 Same as in Fig. 12 but for the Graswang EC site

14). The shape of the mean half-hourly flux footprint is highly similar to that of the wind-rose diagram for that area (See Fig. 1 for the map). It is worth mentioning that the mean flux footprint did not vary significantly between the four seasons, neither in size nor shape. Thus, the figures were excluded for further interpretations.

4 Summary

This study analyzed the turbulent flux variability and EBC in the TERENO prealpine region. We found that the Bowen ratios were mostly positive but small in magnitude due to a high contribution of LE to the surface energy balance during the warm periods. The main reason for the sudden drops of the soil moisture levels was probably related to quick changes in the groundwater level. The PCA results revealed that, based on PC1 (that holds the highest variation of the dataset), the turbulent flux variability is strongly driven by the radiation components of R_n (with an average contribution of approximately 15%) and PPF (14.5%) followed by the temperature variables of SurfaceT (14.3%), AirT (14%) and SoilT (13%) at the study sites. For PC2, however, the dominant contributing variables were WindS (50%) and WindD (35%). Other meteorological variables like albedo, Prec, and RH correlate negatively with different magnitudes across the study area. Furthermore, the monthly diurnal turbulent fluxes of H and LE indicated significant intra-annual variability across the different environments due to the variations of the radiation components, precipitation events, soil moisture and texture, as well as different landscapes in the region. Besides, the highest seasonal diurnal variation observed was for R_n , followed by LE and H , while the lowest one was found for G .

The surface EBC remained unclosed at the EC sites. The EBR values were 0.68, 0.56, and 0.73 at the Fendt, Rottenbuch, and Graswang sites, respectively. The mean imbalance was approximately 35%. The lowest EBR at the Rottenbuch site is partially due to the advection of heat and vapor caused by the heterogeneity of the land surface in that area leading to an underestimation of turbulent fluxes, which somehow substantiated by the flux footprint analysis. The EBC was poor during nighttime periods mainly due to the weak turbulence mixing at night. Overall, the EBC was better in the early afternoon than in the morning (due to the neglected storage terms) with the highest and the lowest EBC at the Graswang and Rottenbuch EC sites, respectively. On average, the annual mean energy balance residual and EBR were 60 W/m^2 and 65%, respectively, in the region. In addition, the size and shape of the flux footprint climatologies were calculated. Approximately 80, 75, and 90% of the annual mean half-hourly turbulent flux footprints received by the instruments from the grassland targets 1 and 2 located at a radius of approximately 250 m around the Fendt, Rottenbuch, and

Graswang stations, respectively. The overall shape of the flux footprints significantly matches the direction of the prevailing winds at the study EC sites.

The knowledge of turbulent flux variability at different time scales and the general EBC problem at the TERENO prealpine region can be significantly strengthened by the results obtained in this research. However, improving the EBC over the region needs further investigation, e.g., by the high resolution large-eddy simulations (LES), for a better understanding of the small-scale weather circulation processes and the environmental conditions over the individual EC sites.

Acknowledgements This research was financially supported by the Helmholtz Research School on Mechanisms and Interactions of Climate Change in Mountain Regions (MICMoR). Access to TERENO and TERENO-ICOS infrastructures is gratefully acknowledged. The support by the landowners of the TERENO sites and technical staff of KIT/IMK-IFU is appreciated, as well. Matthias Mauder's contribution was conducted within the Helmholtz Young Investigator Group "Capturing all relevant scales of biosphere-atmosphere exchange—the enigmatic energy balance closure problem," which is funded by the Helmholtz-Association through the President's Initiative and Networking Fund. We thank Matthias Zeeman (KIT/IMK-IFU) for providing the grass-cuts information related to the management of the grassland sites at the TERENO prealpine region. We are also grateful to Jamie Smidt (KIT/IMK-IFU) for proofreading the manuscript.

References

- Abdi H, Williams LJ (2010) Principal component analysis, WIREs computational statistics, Volume 2, July/August 2010. doi: [10.1002/wics.101](https://doi.org/10.1002/wics.101)
- Aubinet M, Grelle A, Ibrom A, Rannik Ü, Moncrieff J, Foken T et al (1999) Estimates of the annual net carbon and water exchange of forest: the EUROFLUX methodology. *Adv Ecol Res* 30:113–175
- Aubinet M, Vesala T, Papale D (2012) Eddy Covariance - A Practical Guide to Measurement and Data Analysis. Springer, Dordrecht. doi: [10.1007/978-94-007-2351-1](https://doi.org/10.1007/978-94-007-2351-1)
- Baldocchi DD, Hicks BB, Meyers TP (1988) Measuring biosphere-atmosphere exchanges of biologically related gases with micrometeorological methods. *Ecology* 69:1331–1340
- Baldocchi DD, Falge E, Gu LH et al (2001) Fluxnet: a new tool to study the temporal and spatial variability of ecosystem-scale carbon dioxide, water vapor, and energy flux densities. *B Am Meteorol Soc* 82(2415–2434):2001
- Berry JF, Dennison MS (1993) Wetland mitigation. In: Dennison MS, Berry JF (ed) *Wetlands: Guide to Science, Law, and Technology*. Noyes Publications, Park Ridge, pp 278–303
- Blanken PD, Black TA, Yang PC, Newmann HH, Nesic Z, Staebler R, denHartog G, Novak MD, Lee X (1997) Energy balance and canopy conductance of a boreal aspen forest: partitioning overstory and understorey components. *J Geophys Res* 102(D24):28915–28928
- Burba G (2013) Eddy covariance method for scientific, industrial, agricultural and regulatory applications. LI-COR Biosciences, Lincoln
- Burba GG, Verma SB, Kim J (1999) Surface energy fluxes of *Phragmites australis* in a prairie wetland. *Agric For Meteorol* 94(31–51):1999
- Cava D, Contini D, Donato A, Martano P (2008) Analysis of short-term closure of the surface energy balance above short vegetation. *Agric For Meteorol* 148:82–93

- Culf AD, Foken T, Gash JHC (2004) The energy balance closure problem. In: Kabat P, Claussen M et al (eds) *Vegetation, water, Humans and the Climate. A New Perspective on an Interactive System*. Springer, Berlin, Heidelberg, pp 159–166. doi:10.1007/978-3-642-18948-7_13
- De Vries DA (1963) Thermal properties of soils. In: Van Wijk WR (ed) *Physics of plant environment*. North-Holland Publishing Company, Amsterdam, pp 210–235
- Dray S (2008) On the number of principal components: a test of dimensionality based on measurements of similarity between matrices. *Comput Stat Data Anal* 52(2008):2228–2237. doi:10.1016/j.csda.2007.07.015
- Du R, Lu D, Wang G (2006) Diurnal, seasonal, and inter-annual variations of N₂O fluxes from native semi-arid grassland soils of Inner Mongolia. *Soil Biol Biochem* 38:3474–3482
- Eder F, De Roo F, Kohnert K, Desjardins RL, Schmid HP, Mauder M (2014) Evaluation of two energy balance closure parameterizations. *Bound-Layer Meteorol* 151(2):195219
- Foken T (2009) *Micrometeorology*. Springer-Verlag, Berlin Heidelberg. doi:10.1007/978-3-540-74666-9
- Foken T, Oncley SP (1995) Results of the workshop “instrumental and methodical problems of land surface flux measurements”. *Bull Am Meteorol Soc* 76(1191–1193):1995
- Foken T, Wichura B (1996) Tools for quality assessment of surface-based flux measurements. *Agric For Meteorol* 78:83–105
- Foken T, Kukharets VP, Perepelkin VG, Tsvang LR, Richter SH, Weisensee U (1999) “The influence of the variation of the surface temperature on the closure of the surface energy balance,” 13th Symposium on Boundary Layer and Turbulence, Dallas, TX, 10–15 Jan 1999. *Am Meteorol Soc* 308–309:1999
- Foken T, Gockede M, Mauder M, Mahrt L, Amiro BD, Munger JW (2004) Post-field data quality control. In: Lee X, Massman WJ, Law B (ed) *Handbook of micrometeorology: a guide for surface flux measurement and analysis*. Kluwer, Dordrecht, pp 181–208
- Foken T et al (2010) Energy balance closure for the LITFASS2003 experiment. *Theor Appl Climatol* 101:149–160
- Foken T, Aubinet M, Finnigan J, Leclerc M.Y., Mauder M, Tha Paw U, K., (2011) Results of a panel discussion about the energy balance closure correction for trace gases, *Bull Am Meteorol Soc* Doi:10.1175/2011BAMS3130.1
- Gao Z, Horton R, Liu HP, Wen J, Wang L (2009) Influence of wave phase difference between surface soil heat flux and soil surface temperature on land surface energy balance closure. *Hydrol Earth Syst Sci Discuss* 6(1089–1110):2009
- Gurjanov AE, Zubkovskij SL, Fedorov MM (1984) Mnogokanalnaja avtomatizirovannaja sistema obrabotki signalov na baze EVM. *Geod Geophys Veroff R II* 26:17–20
- Hao Y, Wang Y, Huang X, Cui X, Zhou X, Wang S, Niu H, Jiang G (2007) Seasonal and interannual variation in water vapor and energy exchange over a typical steppe in Inner Mongolia, China. *Agric For Meteorol* 146:57–69
- Harazono Y, Kim J, Miyata A, Choi T, Yun J, Kim JW (1998) Measurement of energy budget components during the International Rice Experiment (IREX) in Japan. *Hydrol PRO* 12: 2081–2092. doi:10.1002/(SICI)1099-1085(19981030)12:13/14<2081::AID-HYP721>3.0.CO;2-M
- Hendricks Franssen HJ, Stöckli R, Lehner I, Rotenberg E, Seneviratne SII (2010) Energy balance closure of eddy-covariance data: a multisite analysis for European FLUXNET stations. *Agric For Meteorol* 150: 1553–1567. doi:10.1016/j.agrformet.2010.08.005
- Hingerl L, Kunstmann H, Wagner S, Mauder M, Bliefernicht J, Rigon R (2016) Spatio-temporal variability of water and energy fluxes – a case study for a mesoscale catchment in pre-alpine environment. *Hydrol Process* 30:3804–3823
- Horst TW (1999) The footprint for estimation of atmosphere-surface exchange fluxes by profile techniques. *Bound-Layer Meteorol* 90(171–188):1999
- Hui D, Wan SH, Su B, Katul G, Monson R, Luo Y (2004) Gap-filling missing data in eddy covariance measurements using multiple imputation (MI) for annual estimations. *Agric For Meteorol* 121:93–111
- Imukova K, Ingwersen J, Hevart M, Streck T (2016) Energy balance closure on a winter wheat stand: comparing the eddy covariance technique with the soil water balance method. *Biogeosciences* 13: 63–75. doi:10.5194/bg-13-632016
- Jolliffe I (2002) *Principal component analysis*, second edn. Springer, Berlin
- Kabat P, Claussen M, Dirmeyer PA, Gash JHC, Bravo de Guenni L, Meybeck M, Pielke Sr RA, Vorosmarty CJ, Hutjes RWA, Sutkemeier S (2003) *Vegetation, water, humans and the climate: a new perspective on an interactive system*. The IGBP Series. Springer, Heidelberg, p 650
- Kahan DS, Xue Y, Allen SJ (2006) The impact of vegetation and soil parameters in simulations of surface energy and water balance in the semi-arid sahel: a case study using SEBEX and HAPEX-Sahel data. *J Hydrol* 320:238–259
- Kaimal JC, Finnigan JJ (1994) *Atmospheric boundary layer flows: their structure and measurement*. Oxford University Press, New York 289 p
- Kunstmann H, Schneider K, Forkel R, Knoche R (2004) Impact analysis of climate change for an alpine catchment using high resolution dynamic downscaling of ECHAM4 time slices. *Hydrol Earth Syst Sci* 8(6):1030–1044
- Kunstmann H, Krause J, Mayr S (2006) Invers distributed hydrological modeling of alpine catchments. *Hydrol Earth Syst Sci* 10:395–412
- Kunstmann H, Hingerl L, Mauder M, Wagner S, Rigon R (2013) A combined water and energy flux observation and modelling study at the TERENO-preAlpine observatory, in *Climate and Land-surface Changes in Hydrology*. In: Kunstmann H, Boegh E, Blyth E, Hannah DM, Hisdal H, Su B, Yilmaz KK (ed) *Proceedings of H01, IAHS-IAPSO-IASPEI Assembly, Gothenburg, Sweden, July 2013, IAHS Publ.* 359, pp 221–225
- Lamaud E, Ogée J, Brunet Y, Berbigier P (2001) Validation of eddy flux measurements above the understorey of a pine forest. *Agric For Meteorol* 106:187–203
- Launiainen S, Rinne J, Pumpanen J, Kulmala L, Kolari P, Keronen P, Siivola E, Pohja T, Hari P, Vesala T (2005) Eddy covariance measurements of CO₂ and sensible and latent heat fluxes during a full year in a boreal pine forest trunk-space. *Boreal Environ Res* 10:569–588 ISSN 1239-6095
- Lay D (2012) *Linear algebra and its applications*, 4th ed., Pearson
- Lee X, Hu X (2002) Forest-air fluxes of carbon, water and energy over non-flat terrain. *Bound-Layer Meteorol* 103:277–301
- Lee X, Massman WJ, Law B (2004) *Handbook of micrometeorology: a guide for surface flux measurement and analysis*. Kluwer, Dordrecht 250 pp
- Li W, Hiyama T, Kobayashi N (2013) Seasonal variations of the surface fluxes and surface parameters over the loess plateau in China. *Atmos Clim Sci* 2013(3):111–120
- Liebenthal C, Huwe B, Foken T (2006) Sensitivity analysis for two ground heat flux calculation approaches. *Agric For Meteorol* 132(2005): 253–262. doi:10.1016/j.agrformet.2005.08.001
- Mauder M, Foken T (2006) Impact of post-field data processing on eddy covariance flux estimates and energy balance closure. *Meteorol Z* 15:597–609
- Mauder M, Foken T (2015) *Documentation and instruction manual of the eddy covariance software package TK3 (update) Arbeitsergebnisse*, Univ Bayreuth, Abt Mikrometeorol, Nr. 62, Bayreuth, Juli 2015

- Mauder MC, Liebethal M, Göckede J, Leps F, Beyrich T, Foken (2006) Processing and quality control of flux data during LITFASS2003. *Boundary-Layer Meteorol* 121:67–88
- Mauder M, Jegede O, Okogbue EC, Wimmer F, Foken T (2007) Surface energy balance measurements at a tropical site in West Africa during the transition from dry to wet season. *Theor Appl Climatol* 89:171–183. doi:10.1007/s00704-006-0252-6
- Mauder M, Cuntz M, Drüe C, Graf A, Rebmann C, Schmid HP, Schmidt M, Steinbrecher R (2013) A strategy for quality and uncertainty assessment of long-term eddy-covariance measurements. *Agric For Meteorol* 169:122–135
- Merquioli E, Pnueli L, Cohen M, Simovitch M, Rachmilevitch S, Goloubinoff P, Kaplan A, Mittler R (2002) Seasonal and diurnal variations in gene expression in the desert legume *Retama raetam*. *Plant Cell Environ* 25:1627–1638
- Meyers TP, Hollinger SE (2004) An assessment of storage terms in the surface energy balance of maize and soybean. *Agric For Meteorol* 125:105–115
- Moderow U, Aubinet M, Feigenwinter C, Kolle O, Lindroth A, Mölder M, Montagnani L, Rebmann C, Bernhofer C (2009) Available energy and energy balance closure at four coniferous forest sites across Europe. *Theor Appl Climatol* 98:397–412. doi:10.1007/s00704-009-0175-0
- Moore BCJ (1986) Parallels between frequency selectivity measured psychophysically and in cochlear mechanics. *Stand Audiol Suppl* 25: 139–152
- Nakai T, van der Molen MK, Gash JHC, Kodama Y (2006) Correction of sonic anemometer angle of attack errors. *Agric For Meteorol* 136: 19–30
- Oncley SP, Foken T, Vogt R, Kohsiek W, DeBruin HAR, Bernhofer C, Christen A, van Gorsel E, Grantz D, Feigenwinter C, Lehner I, Liebethal C, Liu H, Mauder M, Pitacco A, Ribeiro L, Weidinger T (2007) The energy balance experiment EBEX2000. Part I: overview and energy balance. *Bound-Layer Meteorol* 123:1–28
- Ott I, Duethmann D, Liebert J, Berg P, Feldmann H, Ihringer J, Kunstmann H, Merz B, Schädler G, Wagner S (2013) High resolution climate change impact analysis on medium sized river catchments in Germany: an ensemble assessment. *J Hydrometeorol* 14(4):1175–1193
- Panin GN, Bernhofer C (2008) Parameterization of turbulent fluxes over inhomogeneous landscapes. *Izv Atmos Ocean Phys* 44:701–716
- Panin GN, Tetzlaff G, Raabe A, Schonfeld HJ, Nasonov AE (1996) Inhomogeneity of the land surface and the parameterization of surface fluxes – a discussion. *Wiss Mitt Inst Meteorol Univ Leipzig und Inst Troposphärenforschung Leipzig* 4:204–215
- Panin GN, Tetzlaff G, Raabe A (1998) Inhomogeneity of the land surface and problems in the parameterization of surface fluxes in natural conditions. *Theor Appl Climatol* 60:163–178
- Pütz T, Kiese R, Wollschläger U, Groh J, Rupp H, Zacharias S, Priesack E, Gerke HH, Gasche R, Bens O, Borg E, Baessler C, Kaiser K, Herbrich M, Munch J-C, Sommer M, Vogel H-J, Vanderborcht J, Vereecken H (2016) TERENO-SOILCan: a lysimeter-network in Germany observing soil processes and plant diversity influenced by climate change. *Environ Earth Sci* 75:1242. doi:10.1007/s12665-016-6031-5
- R Core Team (2017) R: A language and environment for statistical computing. R Foundation for Statistical Computing, Vienna ISBN 3–900051–07–0, URL <http://www.R-project.org/>
- Sanchez JM, Caselles V, Rubio EM (2010) Analysis of the energy balance closure over a FLUXNET boreal forest in Finland. *Hydrol Earth Syst Sci* 14:1487–1497. doi:10.5194/hess-14-1487-2010
- Schmid HP (1994) Source areas for scalars and scalar fluxes. *Bound-Layer Meteorol* 67:293–318
- Schmid HP (1997) Experimental design for flux measurements: matching scales of observations and fluxes. *Agric For Meteorol* 87:179–200
- Schmidt A, Hanson C, Kathilankal J, Law BE (2011) Classification and assessment of turbulent fluxes above ecosystems in North-America with self-organizing feature map networks. *Agric For Meteorol* 151(2011):508–520
- Schotanus P, Nieuwstadt FTM, Bruin HD (1983) Temperature-measurement with a sonic anemometer and its application to heat and moisture fluxes. *Bound-Layer Meteorol* 26(1983):81–93
- Steven JH, Walter CO, Arturo MM (2005) Diurnal, seasonal and annual variation in the net ecosystem CO₂ exchange of a desert shrub community (Sarcocaulis) in Baja California, Mexico. *Glob Chang Biol* 11:927–939
- Stoy PC, Mauder M, Foken T, Marcolla B, Boegh E, Ibrom A, Arain MA, Arneth A, Aurela M, Bernhofer C, Cescatti A, Dellwik E, Duce P, Gianelle D, van Gorsel E, Kiely G, Knohl A, Margolis H, Mccaughy H, Merbold L, Montagnani L, Papale D, Reichstein M, Saunders M, Serrano-Ortiz P, Sottocornola M, Spano D, Vaccari F, Varlagin A, Mccaughy J, Merbold L, Montagnani L, Papale D, Reichstein M, Serrano-Ortiz P, Sottocornola M, Saunders M, Spano D, Vaccari F, Varlagin A (2013) A data-driven analysis of energy balance closure across FLUXNET research sites: the role of landscape-scale heterogeneity. *Agric For Meteorol* 171–172:137–152. doi:10.1016/j.agrformet.2012.11.004
- Stull RB (1988) An introduction to boundary layer meteorology. Kluwer Acad. Publ, Dordrecht 666 pp
- Su Z, Timmermans W, Gieske A, Jia L, Elbers JA, Olioso A, Timmermans J, Van Der Velde R, Jin X, Van Der Kwast H, Nerry F, Sabol D, Sobrino JA, Moreno J, Bianchi R (2008) Quantification of land-atmosphere exchanges of water, energy and carbon dioxide in space and time over the heterogeneous Barrax site. *Int J Remote Sens* 29(17):5215–5235
- Swinbank WC (1951) The measurement of vertical transfer of heat and water vapour by eddies in the lower atmosphere. *J Meteorol* 8:135–145. doi:10.1175/1520-0469(1951)
- Turnipseed AA, Blanken PD, Anderson DE, Monson RK (2002) Energy budget above a high-elevation subalpine forest in complex topography. *Atmos Environ* 110:177201
- Unteregelsbacher S, Gasche R, Lipp L, Sun W, Kreyling O, Geitlinger H, Kogel-Knabner H, Papen H, Kiese R, Schmid HP, Dannenmann M (2013) Increased methane uptake but unchanged nitrous oxide flux in montane grasslands under simulated climate change conditions. *Eur J Soil Sci* 64:586–596. doi:10.1111/ejss.12092
- Verma SB (1990) Micrometeorological methods for measuring surface fluxes of mass and energy. *Remote Sens Rev* 5:99–115
- Wang G, Huang J, Guo W, Zuo J, Wang J, Bi J, Huang Z, Shi J (2010) Observation analysis of land-atmosphere interactions over the Loess Plateau of northwest China. *J Geophys Res* 115:D00K17. doi:10.1029/2009JD013372
- Wang C, Dannenmann M, Meier R, Butterbach-Bahl K (2014) Inhibitory and side effects of acetylene (C₂H₂) and sodium chlorate (NaClO₃) on gross nitrification, gross ammonification and soil-atmosphere exchange of N₂O and CH₄ in acidic to neutral montane grassland soil. *Eur J Soil Biol* 65:7e14
- Webb EK, Pearman GI, Leuning R (1980) Correction of flux measurements for density effects due to heat and water vapour transfer. *Quart J R Meteorol Soc* 106:85–100
- Wei MY (1995) Soil moisture: report of a workshop held in Tiburon, California. NASA Conf Publ, 3319, 80 pp.
- Wicke W, Bernhofer C (1996) Energy balance comparison of the Hartheim Forest and an adjacent grassland site during the HartX Experiment. *Theor Appl Climatol* 53(49–58):1996
- Wilczak JM, Oncley S, Stage S (2001) Sonic anemometer tilt correction algorithms. *Bound-Layer Meteorol* 99:127–150
- Wilson K, Goldstein A, Falge E, Aubinet M, Baldocchi D, Berbigier P, Bernhofer C, Ceulemans R, Dolman H, Field C, Grelle A, Ibrom A, Law BE, Kowalski A, Meyers T, Moncrieff J, Monson R, Oechel W,

- Tenhunen J, Valentini R, Verma S (2002) Energy balance closure at FLUXNET sites. *Agric For Meteorol* 113(1):223–243
- Wizemann HD, Ingwersen J, Högy P, Warrach-Sagi K, Streck T, Wulfmeyer V (2014) Three year observations of water vapor and energy fluxes over agricultural crops in two regional climates of Southwest Germany. *Meteorol Zeitschrift* 24:39–59. doi:10.1127/metz/2014/0618
- Wofsy SC, Goulden ML, Munger JW (1993) Net exchange of CO₂ in a mid-latitude forest. *Science* 260:1314–1317
- Wohlfahrt G, Irschick C, Thkinger B, Hortnagl L, Obojes N, Hammerle A, (2010) Insights from independent evapotranspiration estimates for closing the energy balance: a grassland case study. *Soil Sci Soc Am.* 5585 Guilford Rd. Madison, WI 53711 USA. Doi:10.2136/vzj2009.0158
- Wolf B, Chwala C, Fersch B, Garvelmann J, Junkermann W, Zeeman M, Angerer A, Adler B, Beck C, Brosy C, Brugger P, Emeis S, Dannenmann M, De Roo F, Diaz-Pines E, Haas E, Hagen M, Hajnsek I, Jacobeit J, Jadghuber T, Kalthoff N, Kiese R, Kunstmann H, Kosak O, Krieg R, Malchow C, Mauder M, Merz R, Notarnicola C, Philipp A, Reif W, Reineke S, Rödiger T, Ruehr N, Schäfer K, Schrön M, Senatore A, Shupe H, Voelksch I, Wanninger C, Zacharias S, Schmid H (2017) The ScaleX campaign: scale-crossing land-surface and boundary layer processes in the TERENO-prealpine observatory. *Bull Amer Meteor Soc* 98:1217–1234. doi:10.1175/BAMS-D-15-00277.1
- Wyngaard JC (1990) Scalar fluxes in the planetary boundary layer—theory, modeling, and measurement. *Bound-Layer Meteorol* 50(1–4):49–75. doi:10.1007/BF00120518
- Xu T, Liang S, Liu S (2011) Estimating turbulent fluxes through assimilation of geostationary operational environmental satellites data using ensemble Kalman filter. *J Geophys Res* 116:D09109. doi:10.1029/2010JD015150
- Zeeman MJ, Mauder M, Steinbrecher R, Heidbach K, Eckart E, Schmid HP (2017) Reduced snow cover affects productivity of upland temperate grasslands. *Agric For Meteorol* 232:514–526. doi:10.1016/j.agrformet.2016.09.002